



# Probabilistic Seismic Hazard Maps of Alaska

by Robert L. Wesson<sup>1</sup>, Arthur D. Frankel<sup>1</sup>, Charles S. Mueller<sup>1</sup>, and  
Stephen C. Harmsen<sup>1</sup>

Open-File Report 99-36

1999

This report is preliminary and has not been reviewed for conformity with the U.S. Geological Survey editorial standards or with the North American Stratigraphic Code. Any use of trade, firm or product names is for descriptive purposes only and does not imply endorsement by the U.S. Government.

U.S. DEPARTMENT OF THE INTERIOR  
U.S. GEOLOGICAL SURVEY

<sup>1</sup> Denver, Colorado

## Abstract

Probabilistic seismic hazard maps have been prepared for Alaska portraying ground motion values (peak ground acceleration and spectral amplitude at periods of 0.2, 0.3 and 1.0 seconds) at probabilities of exceedance of 2% and 10% in 50 years. Preparation of these maps followed the same general strategy as that followed for the U.S.G.S. seismic hazard maps of the contiguous United States, combining hazard derived from spatially-smoothed historic seismicity with hazard from fault-specific sources. Preparation of the Alaska maps presented particular challenges in characterizing the hazard from the Alaska-Aleutian megathrust. In the maps of the contiguous United States the rate of seismicity for recognized active faults was determined from slip rates estimated from geologic data. This approach is not appropriate for the megathrust because it has been demonstrated that a significant fraction of the subduction occurs aseismically. The characteristic earthquake hypothesis, based on recurrence rates determined from geologic data, is appealing for the portion of the megathrust that ruptured in the 1964 Alaskan earthquake, but is shown to be inappropriate for the western portion of the megathrust by the recent large earthquakes in the region which did not follow the characteristic model. Consequently the hazard from the western portion was estimated based on a truncated Gutenberg and Richter model derived from historic seismicity, and the hazard for the 1964 zone was estimated from a combination of a Gutenberg and Richter model derived from historic seismicity and the characteristic earthquake hypothesis with recurrence rates estimated from geologic data. Owing to geologic complexity and limited data, hazard models of the easternmost portion of the megathrust in the vicinity of Yakataga are the least satisfactorily constrained. Hazard is estimated for the recognized crustal faults of the Denali, Fairweather-Queen Charlotte and Castle Mountain fault systems based on available geologic slip rates. Hazard from other sources is estimated from spatially smoothed historic seismicity. Disaggregations of the hazard for Anchorage, Fairbanks and Juneau reveal the dominant sources of the hazard at each location.

## Introduction

Alaska is the most seismically active state in the United States, and in 1964 the site of one of the largest earthquakes since the beginning of instrumental recording. Although the current population of the region is small by comparison with, say California, the consequences of a large earthquake in the region could be much greater now than at the time of the 1964 Alaskan earthquake. The probabilistic seismic maps we have prepared are intended to extend those prepared by Frankel et al. (1996) for the 48 contiguous states, and with soon-to-be-published maps for Hawaii. Our methodology follows the basic approach of Cornell (1968). These maps are intended to summarize the available quantitative information about seismic hazard from geologic and geophysical sources. Full color maps at a scale of 1:7,500,000 are available as U.S. Geological Survey Miscellaneous Investigations Series I-2679 (Wesson et al., 1999).

The process of preparing these maps included a workshop held in Anchorage in the fall of 1996 attended by many scientists and engineers involved in aspects of earthquake research and structural engineering practice in Alaska. Preliminary calculations of hazard were presented for discussion and a number of recommendations were made that affected the subsequent preparation of the map. Draft maps were posted on the World Wide Web and circulated for comment in the fall of 1997. The maps presented here have benefited greatly from both the original workshop in 1996 and from the review comments received.

The strategy for preparing these maps is similar to that for recently prepared seismic hazard maps of the contiguous United States (Frankel et al., 1996). The maps presented here include maps for peak ground acceleration and 1.0, 3.3 and 5.0 Hz spectral acceleration at probabilities of exceedance of 10% in 50 years (annual probability of 0.0021) and 2% in 50 years (annual probability of 0.000404).

The historical instrumental seismicity of Alaska and the Aleutians for earthquakes greater than or equal to magnitude 6 is shown in Figure 1. The preparation of the earthquake catalogs used for the analyses in this report (and shown in Figure 1) is discussed in a companion report, Mueller et al., 1998). Clearly the majority of the seismicity in the region is associated with the Alaska-Aleutian megathrust fault extending eastward along the Aleutian arc into south central Alaska. The northwestward-moving Pacific plate is subducted along this megathrust beneath the North American Plate giving rise to the Aleutian trench and islands. Additional significant seismicity occurs along the northwestward-striking system of right-lateral strike-slip faults extending southeastward through and offshore of the panhandle of southeast Alaska. This system of faults forms the northeast boundary of the Pacific plate. Additional seismicity occurs in central Alaska.

The estimated rupture zones of the largest earthquakes in this century are shown in Figure 2 (Plafker et al., 1993). During this century virtually the entire plate boundary from the westernmost Aleutian Islands to the Queen Charlotte Islands off British Columbia has ruptured in large to great earthquakes. The

only exceptions are areas near the Komandorsky Islands, near the Shumagin Islands, and near Cape Yakataga (Sykes, 1971; Davies et al., 1981). Near the Komandorsky Islands, historical records of large earthquakes in 1849 and 1858 at the extreme western end of the arc have been judged as insufficient to conclude that plate-margin-rupturing earthquakes have occurred there (Sykes et al., 1981; Taber et al., 1991). At this location subduction is occurring at a highly oblique angle, and it has been argued that the recurrence properties of large earthquakes here may differ significantly from those else along the arc. Indeed, Cormier (1975) has argued that the region may be incapable of supporting a great earthquake. In the vicinity of the Shumagin Islands, that is, in the region between the 1957 and 1938 earthquakes, it has been argued that no great earthquake has occurred in this century. Similarly, the vicinity of Cape Yakataga has experienced no great earthquakes in this century. These two regions have been identified as "seismic gaps," that is, the potential sites of future large earthquakes (Davies et al., 1981; Sykes, 1971, Lahr et al., 1980).

### **Characterization of Seismic Sources**

The seismic potential of Alaska is captured through consideration of earthquake sources that can be explicitly identified, including the Alaska-Aleutian megathrust and active crustal faults with known slip rates; and earthquake sources that are characterized by spatially smoothed historical seismicity, including shallow earthquakes from sources not included above, and deeper earthquakes (focal depths of 50 to 120 km). Hazard calculated from all these sources was combined as shown in Figure 3. Spatially-smoothed seismicity was used to estimate the hazard from shallow crustal earthquakes in the magnitude range 5.0 to 7.3 based on a Gutenberg-Richter model. For the deeper earthquakes, hazard was estimated for the magnitude range 5.0 to 7.0 based on a Gutenberg-Richter model with the parameters estimated from the spatially-smoothed seismicity in the two depth intervals, 50 to 80 km, and 80 to 120 km.

#### ***Alaska-Aleutian megathrust***

The Alaska-Aleutian megathrust has been responsible for several of the largest earthquakes known in instrumental seismology, including the 1964 Prince William Sound (Mw 9.2) and 1957 Aleutian (Mw 9.1) earthquakes (Figure 2). For purposes of this analysis two different segmentation models of the megathrust with corresponding recurrence assumptions have been considered.

#### **Segmentation models**

In the first segmentation model (Model I), the megathrust has been divided into three parts as shown in Figure 4. The Western Zone includes the reach of the megathrust along the western and central Aleutians from about 170.2° E to 161.7° W. The Eastern Zone extends eastward and includes the reach along the eastern Aleutians, the Alaska Peninsula and Prince William Sound, from about 161.7° W to 144.2° W. Finally, the Yakataga Zone, extends further to the east, across the Copper River delta to Yakutat, that is, to about 139.5° W. In view of the uncertainties in the earthquake potential in the region of the Komandorsky

Islands, no segment of the megathrust was explicitly modeled west of 170.2° E. These boundaries are interpreted to be the limits of the possible rupture surfaces of significant earthquakes associated with the megathrust.

In the second segmentation model of the megathrust (Model II), shown in Figure 5, four segments are considered. This model is similar to the first, in that the Western Zone in Model I generally corresponds to Zone A in Model II, and the Yakataga Zones in the two models are identical. The primary differences between Models I and II arise in the region between the eastern Aleutians and Prince William Sound. In Model II, the Eastern Zone of the Model I is divided into Zones B and C. The portion of the Eastern Zone that ruptured in the 1964 earthquake is identified as Zone C, and the remainder, including the portions of the Eastern Zone that ruptured in the 1938 earthquake and that portion between the 1938 and 1957 earthquake ruptures are included in Zone B.

It seems reasonable to conclude that an earthquake of magnitude 9.2 is the maximum to be expected from the megathrust, but it is not clear whether the potential for an earthquake of this magnitude extends throughout the Eastern Zone of Model I (that is as far west as the limit of the continental crust near 161.7° W), or whether this potential is limited the rupture area of the 1964 earthquake. The occurrence of the 1938 earthquake (Mw 8.2) off the lower Alaskan Peninsula argues that the behavior of this portion of the region may not be characteristic with a magnitude of 9.2. Model II is intended to that this possibility into account, confining the characteristic magnitude 9.2 to the 1964 aftershock zone.

In Model I the boundary between the Western and Eastern zones, and in Model II the boundary between Zones A and B, is taken as the approximate limit of continental crust north of the Aleutian Arc. This segment boundary was suggested by several participants at our workshop. Specifically, we set the boundary at the eastern edge of the 1946 earthquake. The selection of this boundary is based on the assumption that it is extremely unlikely that a large earthquake could rupture through this region. A consequence of prohibiting rupture through a boundary is that the calculated hazard shows a saddle in the region of the boundary. The saddle occurs because the hazard is calculated from a sequence of floating rupture zones that are offset incrementally along the megathrust. Because no rupture zones are allowed to cross the segment boundary, a site at the end of the segment is immediately adjacent to only one floating rupture, and is at increasing distances from all other floating ruptures as they are offset along the megathrust. In contrast, higher hazard is calculated at the center of a segment where a site is immediately adjacent to many floating rupture zones. Reviewers objected to the presence of the saddle, but were unwilling to abandon the concept of a segment boundary in this region. To resolve this incompatibility, in Model I the Western and Eastern Zones were allowed to overlap by 200 km. The resulting hazard is generally constant along the strike of the megathrust through this region. The eastern limit of the Eastern Zone is taken to be the approximate eastern limit of the aftershocks of the 1964 earthquake (and of the well-defined Alaska-Aleutian Benioff zone). The western

boundary of the Western Zone is taken as the western limit of the 1965 Rat Islands earthquake rupture zone (approximately 170° E).

Although a variety of more detailed segmentation models have been proposed for the megathrust zone, large earthquakes, particularly in the western and central Aleutians, notably the 1986 earthquake (Mw 8.0) near Adak Island, have tended to occur without particular regard for the proposed boundaries.

The southern or updip boundaries of the Western and Eastern Zones in Model I and Zones A, B and C in Model II are defined by the so called "seismic front" that is, the presumed updip limit of that part of the megathrust capable of producing a significant earthquake. The seismic front is generally defined by the southern limit of well-recorded seismicity (Engdahl, written communication, 1997) and by the break in slope at the lower edge of the shelf on the northern side of the Aleutian Trench. (This break approximately follows the 400 m depth contour, c.f. Plafker et al., 1993). The updip boundary is taken to be at a depth of 20 km.

The northern or downdip boundaries of the Western and Eastern Zones, except in the area of the Alaskan Peninsula and Cook Inlet, is taken as the 50 km depth contour of earthquakes in the Benioff zone (Plafker et al., 1993). Boyd et al. (1995) observed that standard earthquake locations in the central and western Aleutians are biased as much as several 10's of km to the north, owing to the influence of early arrivals at seismograph stations in Europe to which wave propagation is along anomalously high-velocity paths down the subducting slab. In considering the appropriate northern boundaries of the zones, hypocenters of earthquakes relocated by Engdahl (written communication, 1997) were compared with the map and depth contours of Plafker et al. (1993) and found to be in good agreement. In the eastern Alaskan Peninsula and Cook Inlet regions, the aftershocks of the 1964 earthquake did not extend as far downdip (or north) as the 50 km contour, and the boundary was taken as the approximate northern limit of the aftershocks of the 1964 earthquake (Plafker et al., 1993). In this region the boundary was assumed to lie at a depth 40 km. Between about 155.0° W and 159.2° W the depth to the boundary increases smoothly westward from 40 to 50 km. The assumption about the location of the downdip or northern limit of the megathrust in the Cook Inlet area is important because it significantly affects the estimation of hazard in the area of Anchorage.

Although the Yakataga segment is clearly the location of significant north-south convergence and the site of very large earthquakes (e.g. 1899, 1979) the details of the faulting are poorly understood. Several east-trending, north-dipping thrust faults are inferred to exist beneath the heavily glacier-covered region. As a proxy for a more detailed understanding, a flat fault surface (that is, with a 0° dip) at a depth of 15 km was assumed, extending from 59.1° to 61.0° N and from 139.5° to 145.4° W.

## Recurrence Assumptions

Although the rate of convergence across the Alaska-Aleutian megathrust is relatively well known, the fraction of the convergence that is accommodated by large earthquakes is significantly less than one. This fraction varies with position along megathrust zone, but is poorly known. It appears to range from 10% or less to near 100% (c.f. Pacheco et al., 1993). Thus, estimates of the rate of large earthquakes based on the known convergence rate alone are unrealistically large, well above the observed rate of large earthquakes over the last century.

Other than the plate convergence rate, the only data available to estimate recurrence along the entire megathrust is the instrumental seismicity catalog. At present geologic data for recurrence exists only for the 1964 zone. Plafker and Rubin (1994) estimate that seven or eight events with displacements similar to 1964 are reflected in the stratigraphic sequence in the Copper River delta in the ~5600 years preceding 1964. These data suggest a recurrence time for earthquakes of magnitude 9.2 of 700 to 800 years. The occurrence of the 1938 earthquake (Mw 8.2) off the lower Alaskan Peninsula indicates that very large earthquakes with magnitudes less than 9.2 occur as well. Therefore, one must ask the question, "What is the largest earthquake that might have occurred within the 1964 zone, but would not be reflected in the stratigraphy of the Copper River delta?" Our estimate is that an earthquake with a magnitude as large as 8 could occur without causing sufficient vertical displacement in the region of the Copper River delta to be reflected in the stratigraphy.

In view of the limited geologic data, recurrence assumptions for most of the megathrust are based on instrumental seismic data. Hazard was estimated assuming a Gutenberg-Richter recurrence model for magnitude 7.0 to 9.2 in the Western Zone of Model I and Zone A of Model II. Similarly, a Gutenberg-Richter recurrence model was assumed for magnitudes 7.0 to 8.5 in Zone B of Model II, for magnitudes of 7.0 to 8 in the Eastern Zone of Model I and Zone C of Model II, and for magnitudes 7.0 to 8.1 in the Yakataga Zone. The parameters  $a$  and  $b$  in the Gutenberg-Richter relations was estimated in each of these regions from the historical seismicity data. In addition a characteristic earthquake of magnitude 9.2 with a recurrence time of 750 years was assumed for the Eastern Zone of Model I and for Zone C of Model II.

## Smaller Earthquakes

Hazard for earthquakes in the magnitude range 5.0 to 7.0 was calculated from a Gutenberg-Richter recurrence relation determined for each of the megathrust source zones.  $a$  and  $b$ - values were determined for each of the source zones of the megathrust. These seismicity parameters were determined from maximum-likelihood fits of  $\log N$  versus magnitude for shallow events greater than magnitude 4.5, the minimum magnitude of completeness in the region since 1964. Hazard was calculated using the  $a$ -value and  $b$ -value for each zone. No smoothing was applied to the edges of these source zones. Details may be found in the companion report by Mueller et al. (1998).

## *Active Crustal Faults*

Although considerable information is available about a few active crustal faults in Alaska, there are certainly many more faults with unknown slip rates. Faults included explicitly in the map are shown in Figure 6. (Note that the seismic hazard associated with faults not explicitly included in the map is captured to a large degree by the smoothed seismicity model described below.) To be included in this map a fault must have an estimated slip rate. As in our treatment of western U.S. faults in the national maps (Frankel et al., 1996), we divide the faults into two types: A (characteristic) and B (hybrid). The A-type faults are faults with "known" segmentation. We use a characteristic rupture model for the A-type faults in which rupture occurs only as the largest earthquake estimated for each fault segment. B-type faults have "unknown" segmentation, so we use two equally-weighted recurrence models. For these hybrid faults, we calculated hazard using 50% weight for the characteristic earthquake model and 50% weight for a truncated Gutenberg-Richter frequency-magnitude relation. We used a minimum magnitude of M6.5 and a maximum magnitude of  $M_{char}$  for the Gutenberg-Richter hazard calculation. In general, the Gutenberg-Richter recurrence model yields higher hazard for a given fault than the characteristic model, because of the more frequent occurrence of moderate-sized earthquakes in the Gutenberg-Richter model. Use of this model is intended here to account for the possibility that the crustal faults will rupture in segments smaller than their entire length.

Recurrence times (characteristic) and  $a$ - values (G-R) for the each fault were determined from their slip rates, not from the seismicity surrounding the fault. Characteristic magnitudes were determined from fault lengths using the relations of Wells and Coppersmith (1994). See Frankel et al. (1996) for the formulas deriving the  $a$ - values and characteristic earthquake rates from the geologic slip rate and area of fault. The fault widths of crustal faults were estimated by assuming a maximum faulting depth of 15 km. These crustal faults were taken to be vertical, except for the Castle Mountain fault (dips 75° to North) and the Transition fault (dips 10° to North).

Table 1 identifies the faults (and fault segments) included in the map, and the assumptions made about them. The slip rates are from Nishenko and Jacob (1990) and Plafker et al. (1993) except as noted below. The recurrence times in the table are for the characteristic earthquakes. Again, the hybrid faults also use a Gutenberg-Richter recurrence model which will produce more frequent recurrence for earthquakes between M6.5 and  $M_{char}$ .

Estimates of the slip rate for the Totschunda fault ranged from 8 to 15 mm/yr (Plafker et al., 1993). We adopted a "mean" value of 11.5 mm/yr.

We note that we treated the Transition fault as an A-type fault, even though its segmentation is unknown. In initial hazard calculations using a hybrid approach for this fault, we found that the Transition fault produced the highest hazard in the map. The slip rate of the Transition fault is highly uncertain (J. Lahr, pers. comm.), and we were concerned that one of the more poorly known faults

had a higher hazard than the megathrust zone. Consequently, we used only the characteristic rupture model for the Transition fault, which produces a lower hazard than the hybrid approach. Also, we used the Youngs et al. (1997) subduction zone interface attenuation relation when estimating ground motions for the Transition fault (see attenuation section below). This produces somewhat lower ground motions than do attenuation relations for crustal earthquakes.

Of particular interest is the Castle Mountain fault, passing about 40 km from Anchorage. The fault has been considered in two segments the western, or Susitna segment, and the eastern or Talkeetna, segment (Detterman et al., 1994). Along the Talkeetna segment there is no evidence for surficial displacement younger than Pleistocene (Detterman et al., 1976), but Lahr et al. (1986) describe an earthquake of  $M_s$  5.2 which indicated slip at a depth of 13 to 20 km along the segment. In contrast, along the Susitna segment, no significant earthquakes have been instrumentally located, but geologic studies indicate Holocene surface displacement (Detterman et al., 1974, 1976; Bruhn, 1979). These studies, however, have served only to put wide limits on the slip rate. We chose a value of 0.5 mm/yr and a maximum magnitude of 7.5 leading to a recurrence time of 1300 years (R. Updike, oral communication, 1997).

### **Determination of Seismicity Parameters from Spatially-smoothed Seismicity**

For the smoothed seismicity calculation, the shallow events (focal depth <50 km) in the areal source zones of the megathrust were first removed from the catalog. Next the catalog was divided into shallow, deep (focal depth 50-80 km) and deeper (focal depth 80 to 120 km) events.  $b$ -values were determined separately for the shallow, deep and deeper events using the maximum likelihood method (Weichert, 1980) for events with magnitudes greater than 4.5. We found  $b$ -values of 0.87 for the shallow seismicity, 1.2 for the deep seismicity (50-80 km depth), and 1.15 for the deeper seismicity (80-120 km depth).

Using the approach of Frankel (1995),  $a$ -value grids were calculated using the maximum-likelihood formula from Weichert (1980). These  $a$ -value grids were then smoothed with Gaussian smoothing functions (correlation distance of 75 km) and the hazard was calculated by summing the frequencies of exceedance for all of the grid cells. This was done separately for the shallow and two deep cases. These  $a$ -value grids were then used as the basis to calculate the hazard arising from earthquakes in the magnitude range 5.0 to 7.0 (5.0 to 7.3 for the shallow case).

### **Source Finiteness in Hazard Calculation**

In all the calculations of hazard, the treatment of source finiteness varied with magnitude range. For events between  $M_{5.0}$  and  $M_{6.5}$ , we assumed point sources. For events from  $M_{6.5}$  to  $M_{7.0}$  ( $M_{6.5}$  to  $M_{7.3}$  in the case of shallow earthquakes) we used finite faults of arbitrary strike. For events greater than magnitude 7.0 in the megathrust zone, we used floating rupture zones offset incrementally along the megathrust.

For the crustal faults, when using the Gutenberg-Richter recurrence model, we floated the rupture zones along the fault. The floating rupture zones along the crustal faults and the megathrust cause a tapering of the hazard at the ends of the faults.

### **Attenuation Relationships**

The reference site condition is the NEHRP B/C boundary, which corresponds to an average shear-wave velocity of 760 m/sec in the top 30m. This is the same site condition used in the 1996 national maps. This site condition represents a typical western U.S. "firm-rock" site. Table 2 shows the ground motion relationships used in the calculations. These are the same relations used in producing the 1996 hazard maps for the western U.S. For crustal faults we used different ground motion values for thrust faults and for strike-slip faults, using the values specified in each attenuation study. For the deep earthquakes, we assumed a focal depth of 60 km for earthquakes in the depth interval 50 to 80 km, and a focal depth of 90 km for earthquakes in the depth interval 80 to 120 km.

### **Discussion of Maps**

Probabilistic seismic hazard maps for Alaska calculated as described above are shown in Figures 7-10, for peak ground acceleration, 5.0, 3.3, and 1 Hz spectral acceleration, and for 10% and 2% probability of exceedance in 50 years.

Hazard is highest in the coastal regions adjacent to the megathrust and the Transition Fault and in regions adjacent to the Denali and Fairweather-Queen Charlotte fault systems at all periods and probability levels. In the interior of Alaska, away from the Denali fault, hazard is dominated by the spatially-smoothed seismicity. The region of lowest hazard in Alaska is along the northern coast adjacent to the Arctic Ocean. The hazard associated with the Castle Mountain fault is overwhelmed by the megathrust at most periods and probability levels, but can be seen on the map of peak ground acceleration with 2% probability of exceedance in 50 years (Figure 7b.) In general hazard in the higher hazard regions of Alaska is comparable to areas of higher hazard in California (Frankel et al., 1996).

Disaggregations by magnitude and distance to the source of the hazard are shown in Figures 11, 12 and 13 for Anchorage, Fairbanks and Juneau for peak ground acceleration and 5 Hz and 1 Hz spectral acceleration at the 2%-in-50 year probability level. The disaggregation plots include the summary joint distribution statistics, the mean magnitude and distance ("mbar" and "dbar"), and the modal magnitude and distance ("mmode" and "dmode").

The disaggregations for Anchorage indicate the role of great earthquakes (magnitude 9 at a distance of about 50 km) relative to the other sources (Figure 11). The relative contribution of the great earthquakes increases with increasing period (decreasing frequency) until the great earthquakes dominate at a

frequency of 1 Hz. On these plots hazard from the Castle Mountain fault at a distance of about 40 km is combined with the hazard from earthquakes in the magnitude range up to 7.5 on the megathrust. The other significant contributions to the hazard arise from the shallow smoothed seismicity (shown at a distance of about 20 km) and the two deeper zones of smoothed seismicity (show at distances of 60 and 90 km).

The disaggregations for Fairbanks (Figure 12) show that the hazard is dominated by local earthquakes. The influences of the Denali fault at distance of about 135 km and the megathrust at a distance of about 350 km are only apparent on the disaggregation for 1 Hz.

The disaggregations for Juneau (Figure 13) show the relative contributions of the local shallow seismicity and large earthquakes on the South Denali (Chatham Strait) fault at a distance of about 80 km. The relative contribution of the large earthquakes on the South Denali increase with increasing period (decreasing frequency).

Although somewhat more detailed, the current maps for peak ground acceleration are generally similar to the maps prepared by Thenhaus et al. (1985) for the corresponding probability levels, although significant differences do exist. (Thenhaus et al. did not estimate the hazard in the area of the Aleutian Islands.) In general the values on the current map for the 10%-in-50-year probability level are somewhat lower than those on the Thenhaus et al. map in south central and southeast Alaska, but somewhat higher in the offshore regions above and adjacent to the megathrust. The values on the current 2%-in-50-year map are similar to those on the Thenhaus et al. map in south central and southeast Alaska, but somewhat higher in the offshore regions above and adjacent to the megathrust. For example, for the Anchorage area at the 10%-in-50-year probability level, the current map indicates a peak ground acceleration of 37% g, in contrast to about 45% for the Thenhaus et al. map. At the 2% in 50 year probability level, the current map indicates about 65% g for the Anchorage area, as contrasted with ~67% g on the Thenhaus et al. map. Table 3 compares estimates of the estimated peak ground accelerations from the current maps and the Thenhaus et al. maps at nine locations in Alaska.

### **Conclusions and Issues Requiring Future Work**

Alaska has some of the areas of highest seismic hazard in the United States. In contrast to California where most of the regions of highest hazard occur in relatively narrow zones and are often associated with nearly vertical faults, most of the hazardous regions in Alaska occur in association with relatively shallow dipping faults leading to much larger affected areas. The principal sources of seismic hazard in Alaska are the Alaska-Aleutian megathrust and the Transition fault (both relatively shallow dipping and affecting very large areas), and the Fairweather, Queen Charlotte and Denali faults (near vertical faults leading to relatively narrow zones of high hazard.)

Obviously, there are many aspects of the methodology and input information that can be debated. In constructing these maps we have attempted to include those elements of geologic and geophysical information and interpretation for which a community consensus exists. We have also attempted to indicate explicitly those areas where we have been forced to rely on judgment or assumption.

Future seismic hazard maps would benefit from additional information in several areas. Additional understanding of the characteristics of faulting in subduction zones, especially the 1964 zone would be very helpful. Tectonic understanding of the region between the 1964 zone and the Fairweather fault, including the Yakataga gap and the Transition fault would be extremely valuable. More measurements of slip rates on the crustal faults are needed. Finally, new insights into the segmentation of the megathrust and the expected magnitude distribution of earthquakes would have a large impact.

Specific methodological issues that warrant further consideration include: 1) Segmentation boundaries on faults characterized by large earthquakes cause saddles in hazard with lower hazard near boundary, because of the tapering of hazard caused by floating rupture zones. We dealt with this saddle in the hazard in an ad hoc manner by overlapping the zones. This issue requires additional consideration over the long run. 2) We used historical seismicity rather than convergence rates to establish rates of large ( $M \geq 7$ ) earthquakes in the megathrust source zones. It would be desirable to rationalize the seismicity rates with the convergence rate through some quantitative mechanism. 3) Future segmentation models for the megathrust could benefit greatly from additional tectonic insight. 4) Use of time-dependent probabilities.

### **Acknowledgments**

We thank the participants of the September 1996 workshop on seismic-hazard mapping in Alaska for their valuable suggestions and guidance. Many of their comments were applied to make the draft maps. We particularly thank Max Wyss and Stefan Wiemer of the Geophysical Institute and John Lahr of the USGS for their help with the treatment of earthquake catalogs (see accompanying documentation). George Plafker, Randy Updike, and Don Wells provided useful discussions. C.B. Crouse, K.H. Jacob and E.V. Leyendecker provided helpful reviews. Ken Rukstales prepared the full color 1:7,500,000 scale maps for publication.

### **References**

Boore, D., W. Joyner, and T. Fumal (1997). Equations for estimating horizontal response spectra and peak acceleration from Western North American earthquakes: a summary of recent work, *Seism. Res. Letts.*, v. 68, no. 1, pp. 128-153.

- Boyd, T.M., E.R. Engdahl, and W. Spence, (1995). Seismic cycles along the Aleutian arc: Analysis of seismicity from 1957 through 1991, *J. Geophys. Res.*, v. 100, pp. 621-644.
- Bruhn, R.L. (1979). Holocene displacements measured by trenching the Castle Mountain fault near Houston, Alaska, in *Short Notes on Alaska Geology*, Alaska Division of Geological and Geophysical Surveys, Geologic Report 61, Anchorage, Alaska, 4 p.
- Campbell, K. and Y. Bozorgnia (1994). Near-source attenuation of peak horizontal acceleration from worldwide accelerograms recorded from 1957 to 1993, in *Proceedings of Fifth U.S. National Conference on Earthquake Engineering*, Earthquake Engineering Research Institute, Oakland, California, III, pp. 283-292.
- Cormier, V. (1975). Tectonics near the junction of the Aleutian and Kuril-Kamchatka arcs and a mechanism for the middle Tertiary magmatism in the Kamchatka basin, *Geol. Soc. Amer. Bull.*, v. 86., pp. 443-453.
- Cornell, A. (1968). Engineering seismic risk analysis, *Bull. Seism. Soc. Am.*, v. 58, pp. 1583-1606.
- Davies, J.N., L. R. Sykes, L. House, and K. Jacob (1981). Shumagin seismic gap, Alaskan peninsula: History of great earthquakes, tectonic setting and evidence for high seismic potential, *J. Geophys. Res.*, v. 86, pp. 3821-3855.
- Detterman, R.L., G. Plafker, T. Hudson, R.G. Tysdal, and N. Pavoni (1974). Surface geology and Holocene breaks along the Susitna segment of the Castle Mountain fault, Alaska, *U.S. Geol. Surv. MF Map 618*, 1 sheet.
- Detterman, R.L., G. Plafker, G.T. Russell, and T. Hudson (1976). Features along part of the Talkeetna segment of the Castle Mountain-Caribou fault system, Alaska, *U.S. Geol. Surv. MF Map 638*, 1 sheet.
- Frankel, A. (1995). Mapping seismic hazard in the Central and Eastern United States, *Seism. Res. Letts*, v. 66, no. 4, pp. 8-21.
- Frankel, A., C. Mueller, T. Barnhard, D. Perkins, E. Leyendecker, N. Dickman, S. Hanson, and M. Hopper (1996). National seismic-hazard maps: Documentation June 1996, U.S. Geological Survey Open-File Report 96-532, 110 pages.
- Lahr, J.C., C.D. Stephens, H.S. Hagewara, and J. Boatwright (1980). Alaska seismic gap only partially filled by 28 February 1979 earthquake, *Science*, v207, pp. 1351-1353.
- Lahr, J. , R.A. Page, C.D. Stephens, and K.A. Fogelman (1986). Sutton, Alaska, earthquake of 1984: Evidence for activity on the Talkeetna segment of the Castle Mountain fault system, *Bull. Seism. Soc. Am.*, v. 76, pp. 967-984.
- Mueller, C., A. Frankel, J. Lahr, and M. Wyss (1998). Preparation of earthquake catalogs for the national seismic hazard maps: Alaska, U.S. Geological Survey Open-File Report, in preparation.
- Nishenko, S.P., and K.H. Jacob (1990). Seismic potential of the Queen Charlotte-Alaska-Aleutian-seismic zone, *J. Geophys. Res.*, v. 95, pp. 2511-2532.
- Pacheco, J., L. Sykes, and C. Scholz (1993). Nature of seismic coupling along simple plate boundaries of the subduction type, *J. Geophys. Res.*, v. 98, pp. 14,133-14,159.
- Page, R.A., N.N. Biswas, J.C. Lahr, and H. Pulpan (1991). Seismicity of continental Alaska, in Slemmons, D.B., Engdahl, E.R., Zoback, M.R., and Blackwell, D.D.,

- eds., Neotectonics of North America: Boulder, Colorado, Geol. Soc. Am., Decade Map Volume 1, pp. 47-68.
- Plafker, G., L. Gilpin, and J. Lahr (1993). Neotectonic map of Alaska, in *Geology of Alaska*, vol G-1 of *Geology of North America*, Geological Society of America, Boulder, CO.
- Plafker, G. and M. Rubin, (1994). Paleoseismic evidence for "yo-yo" tectonics above the eastern Aleutian subduction zone: coseismic uplift alternating with even larger interseismic submergence, in *Proceedings of the Workshop on Paleoseismology*, C. S. Prentice, D.P. Schwartz and R.S. Yeats, Convenors, USGS Open-file report 94-568, p.155-157.
- Sadigh, K., C. Chang, J. Egan, F. Makdisi, and R. Youngs (1997). Attenuation relationships for shallow crustal earthquakes based on California strong motion data, *Seism. Res. Letts.*, v. 68, no. 1, pp. 180-189.
- Sykes, L.R. (1971). Aftershock zones of great earthquakes, seismicity gaps, and earthquake prediction for Alaska and the Aleutians, *J. Geophys. Res.*, v. 76, pp. 8021-8041.
- Sykes, L.R., J.B. Kisslinger, L. House, J.N. Davies, and K.H. Jacob (1981). Rupture zones and repeat times of great earthquakes along the Alaska-Aleutian arc, in Simpson D.W. , and R.G. Richards, eds., *Earthquake prediction: American Geophysical Union*, pp. 73-80.
- Taber, J.J., S. Billington, and E.R. Engdahl, (1991). Seismicity of the Aleutian arc, in Slemmons, D.B., Engdahl, E.R., Zoback, M.R., and Blackwell, D.D., eds., *Neotectonics of North America: Boulder, Colorado, Geol. Soc. Am., Decade Map Volume 1*, pp. 29-46.
- Thenhaus, P.C., J.I. Ziony, W.H. Diment, M.G. Hopper, D.M. Perkins, S.L. Hanson, and S.T. Algermissen (1985). Probabilistic estimates of maximum seismic horizontal ground acceleration on rock in Alaska and the adjacent continental shelf, *Earthquake Spectra*, v. 1, pp. 285-306.
- Youngs, R., S. Chiou, W. Silva, and J. Humphrey (1997). Strong ground motion attenuation relationships for subduction zone earthquakes, *Seism. Res. Letts.*, v. 68, no. 1, pp. 58-73.
- Weichert, D. (1980). Estimation of earthquake recurrence parameters for unequal observation periods for different magnitudes, *Bull. Seism. Soc. Am.*, v. 70, pp. 1337-1356.
- Wesson, R.L., A.D. Frankel, C.S. Mueller, S.C. Harmsen (1999). *Seismic-Hazard Maps for Alaska and the Aleutian Islands*. U.S. Geological Survey Miscellaneous Investigations Series I-2679, 2 sheets.

## Figure Captions

Figure 1. Instrumental seismicity of Alaska and the Aleutian Islands from the consolidated catalogs. Earthquakes shown have magnitudes,  $M_w \geq 5.5$ , and dates ranging from 1880 to 1996. (Mueller et al., 1998).

Figure 2. Rupture areas of large earthquakes in the Alaska Aleutian region during this century (Plafker et al., 1993). Note that virtually the entire boundary between the Pacific and North American Plates has ruptured during this period with the exceptions of 1) the western most Aleutians ( $\sim 168^\circ\text{E}$ ), 2) the Shumagin gap ( $\sim 160^\circ\text{W}$ ), and 3) the Yakataga gap ( $\sim 142^\circ\text{W}$ ). See text for discussion.

Figure 3. Hazard Model for Alaska.

Figure 4. Segmentation Model I for the Alaska-Aleutian Megathrust

Figure 5. Segmentation Model II for the Alaska-Aleutian Megathrust

Figure 6. Active crustal faults identified in Alaska (Plafker et al., 1993).

Figure 7a. Peak ground acceleration (%g) with 10% probability of exceedance in 50 years.

Figure 7b. Peak ground acceleration (%g) with 2% probability of exceedance in 50 years.

Figure 8a. 5 Hz acceleration (%g) with 10% probability of exceedance in 50 years.

Figure 8b. 5 Hz acceleration (%g) with 2% probability of exceedance in 50 years.

Figure 9a. 3.3 Hz acceleration (%g) with 10% probability of exceedance in 50 years.

Figure 9b. 3.3 Hz acceleration (%g) with 2% probability of exceedance in 50 years.

Figure 10a. 1 Hz acceleration (%g) with 10% probability of exceedance in 50 years.

Figure 10b. 1 Hz acceleration (%g) with 2% probability of exceedance in 50 years.

Figure 11a. Disaggregation of hazard at Anchorage for peak ground acceleration at 2%-in-50 year probability level.

Figure 11b. Disaggregation of hazard at Anchorage for 5 Hz ground acceleration at 2%-in-50 year probability level.

Figure 11c. Disaggregation of hazard at Anchorage for 1 Hz spectral acceleration at 2%-in-50 year probability level.

Figure 12a. Disaggregation of hazard at Fairbanks for peak ground acceleration at 2%-in-50 year probability level.

Figure 12b. Disaggregation of hazard at Fairbanks for 5 Hz ground acceleration at 2%-in-50 year probability level.

Figure 12c. Disaggregation of hazard at Fairbanks for 1 Hz spectral acceleration at 2%-in-50 year probability level.

Figure 13a. Disaggregation of hazard at Juneau for peak ground acceleration at 2%-in-50 year probability level.

Figure 13b. Disaggregation of hazard at Juneau for 5 Hz ground acceleration at 2%-in-50 year probability level.

Figure 13c. Disaggregation of hazard at Juneau for 1 Hz spectral acceleration at 2%-in-50 year probability level.

## Table Captions

Table 1. Characteristics of active faults assumed for hazard analysis.

Table 2. Attenuation models assumed for various seismic sources assumed for hazard analysis.

Table 3. Comparison of peak ground acceleration for selected locations in Alaska between the current maps and those prepared by Thenhaus et al. (1985).

Figure 1

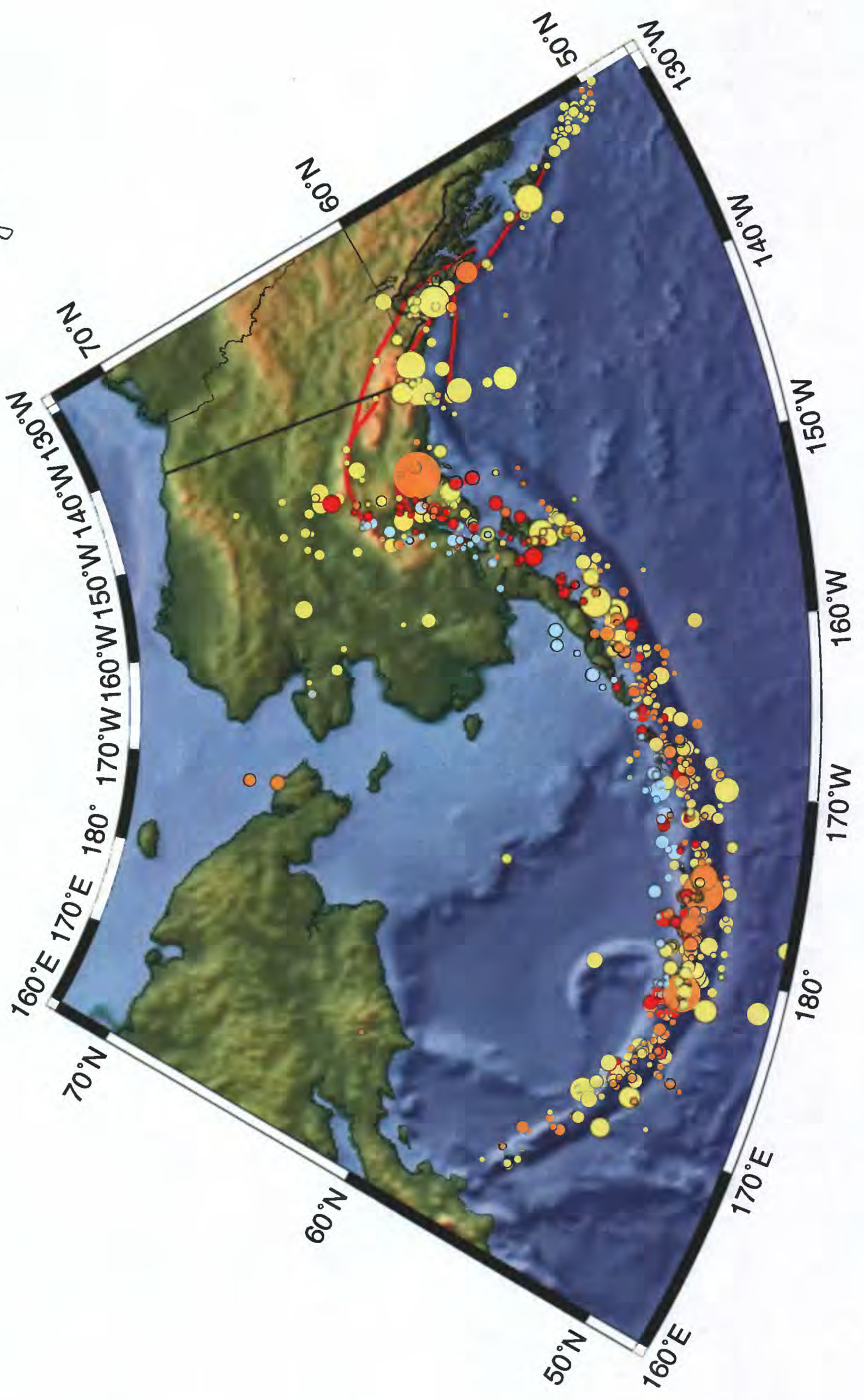


Figure 1

Figure 2

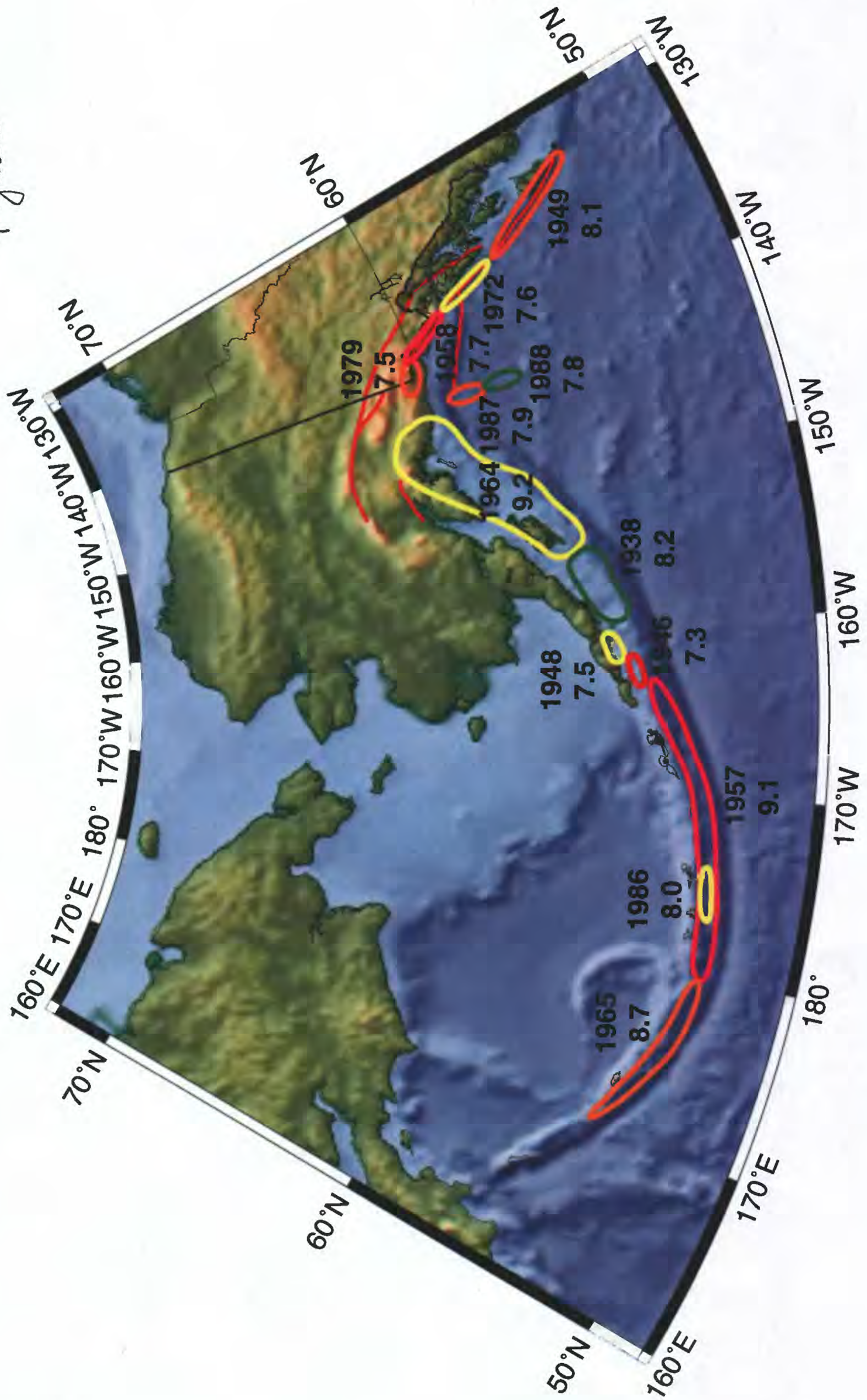


Figure 2

# Hazard Model for Alaska

Figure 3

$5.0 \leq M \leq 7.0^*$

$M \geq 7.0$

## Spatially Smoothed Seismicity

Shallow Earthquakes (0-50 km)  
 $5.0 \leq M \leq 7.3$

Deeper Earthquakes (50-80 km)  
 $5.0 \leq M \leq 7.0$

Deepest Earthquakes (80-120 km)  
 $5.0 \leq M \leq 7.0$

Megathrust source zones  
 $5.0 \leq M \leq 7.0$

## Megathrust Zone

Equal weights on two segmentation models with recurrence rates for truncated Gutenberg-Richter determined from historical seismicity and recurrence rate for Characteristic Model in 1964 zone determined from geologic studies

## Faults with "known" segmentation (A)

Characteristic Model using slip rates to obtain recurrence of maximum earthquake

## Faults with "unknown" segmentation (B)

Equal weights on Characteristic Model and truncated Gutenberg-Richter for 7.0 to maximum magnitude, and using slip rates for recurrence

\*An upper limit of magnitude 7.3 was adopted for the shallow earthquakes to accommodate the possible occurrence of a background earthquake of that magnitude.

Figure 4

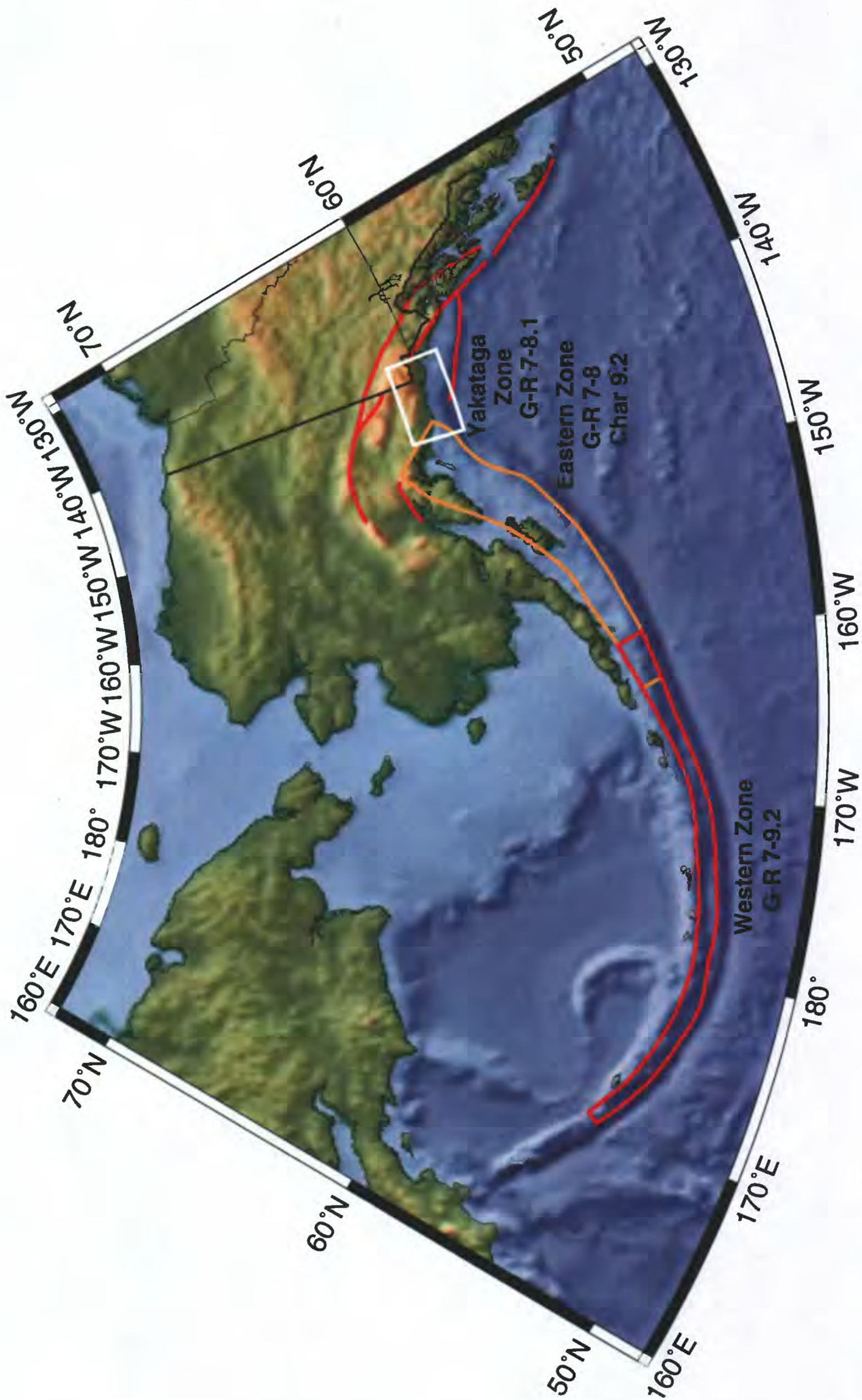


Figure 4

Figures

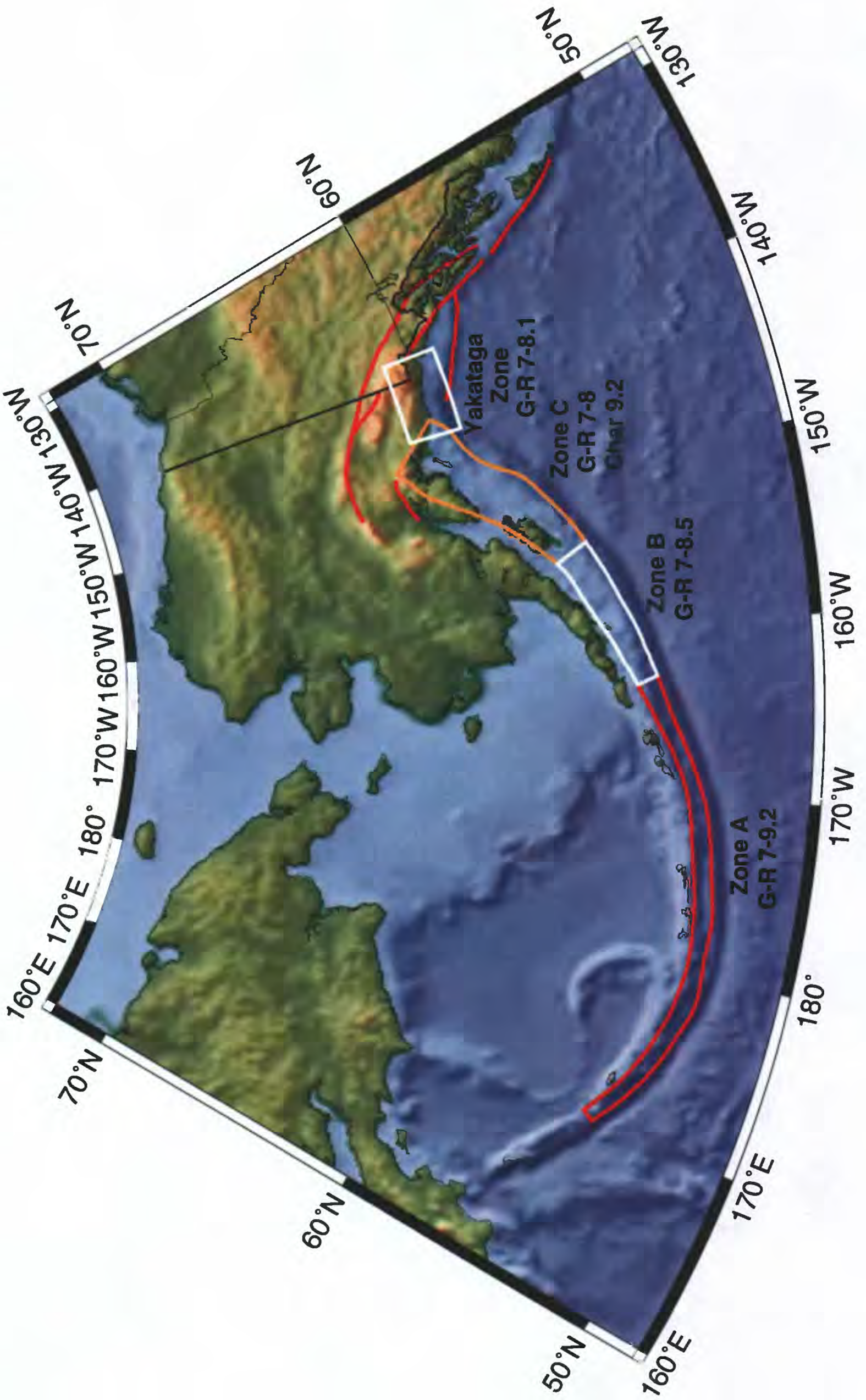


Figure 5

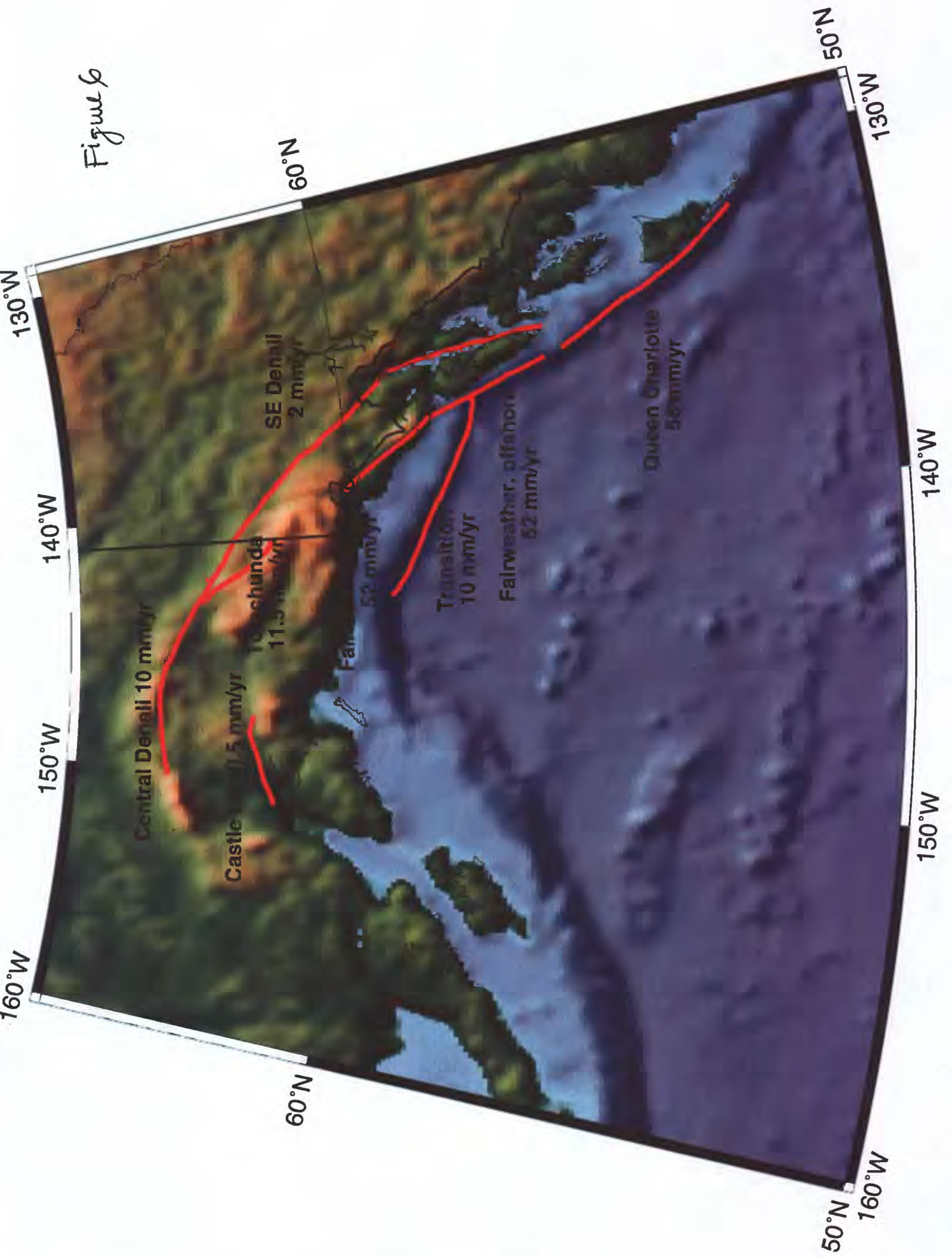
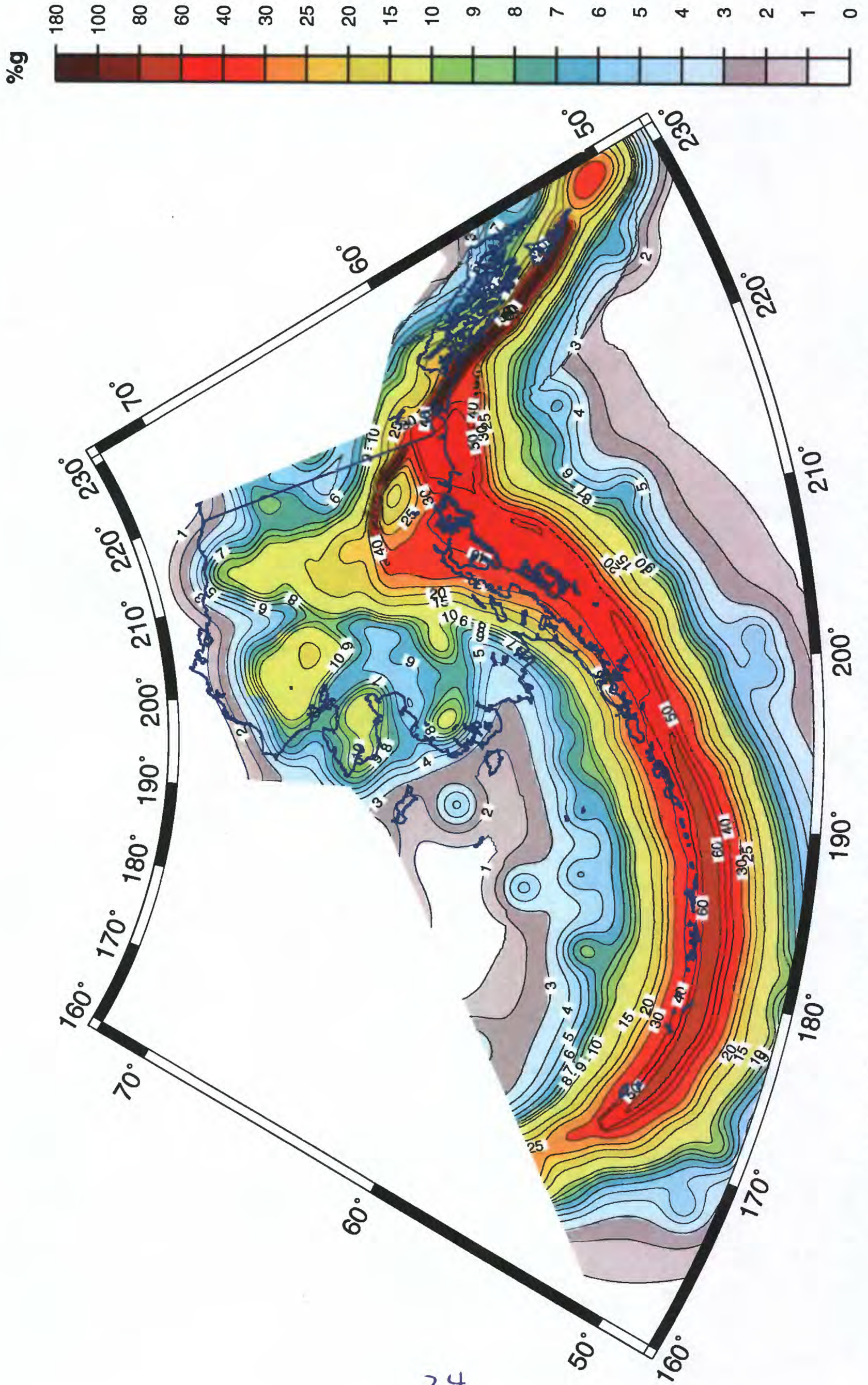


Figure 6

Figure 6

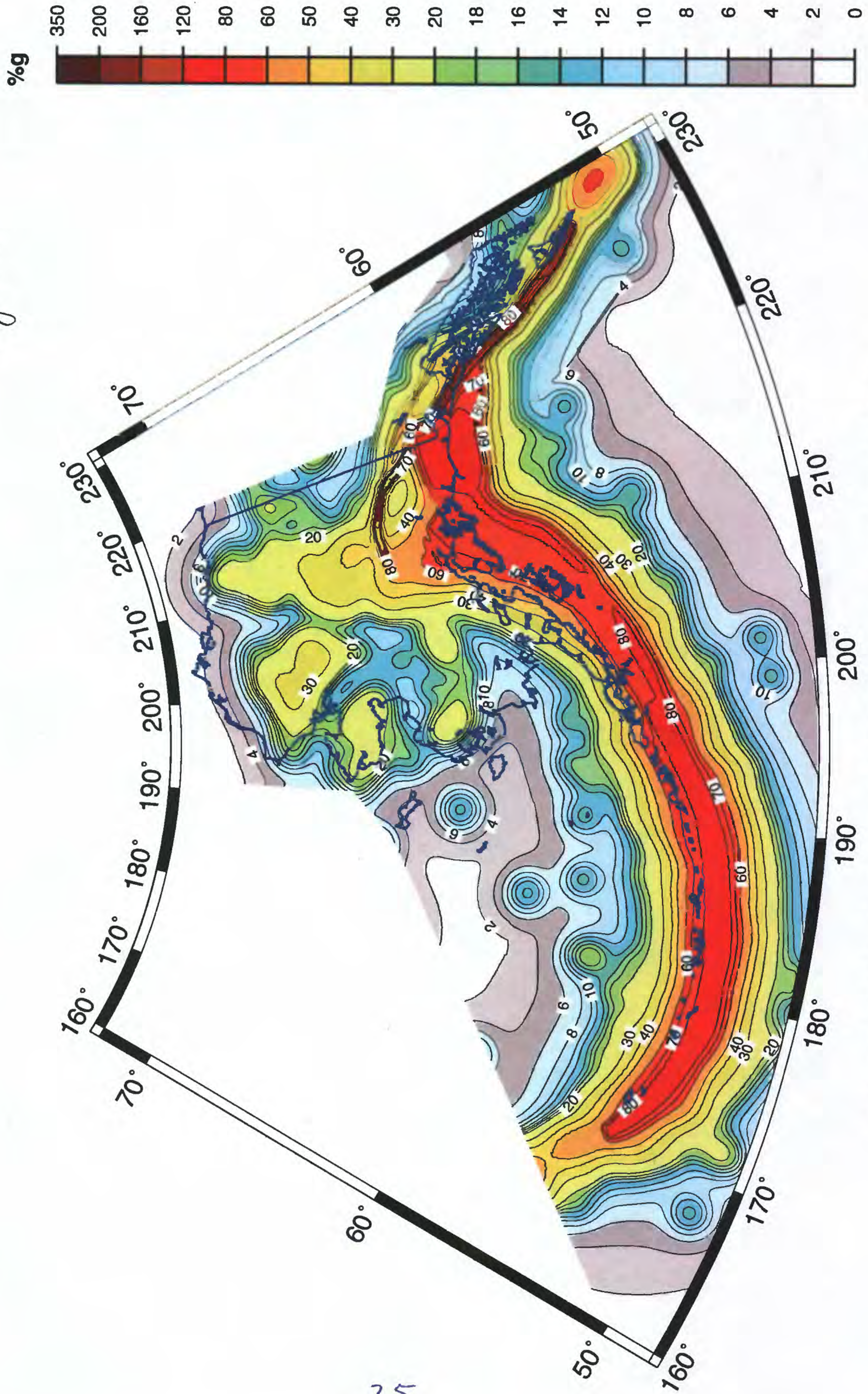
Figure 79



Peak Ground Acceleration (%g) with 10% Probability of Exceedance in 50 Years

Figure 79

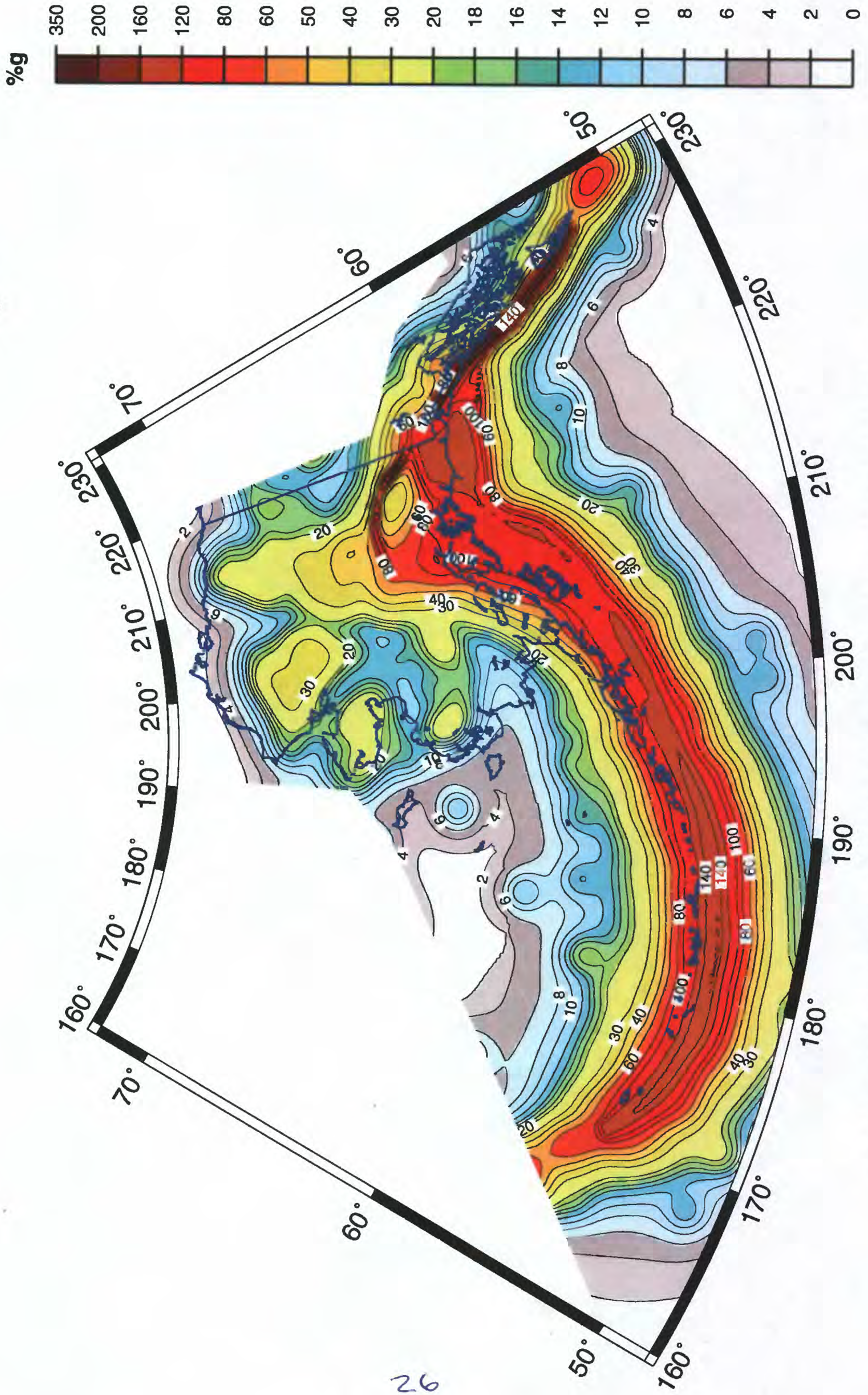
Figure 7b



Peak Ground Acceleration (%g) with 2% Probability of Exceedance in 50 Years

Figure 7b

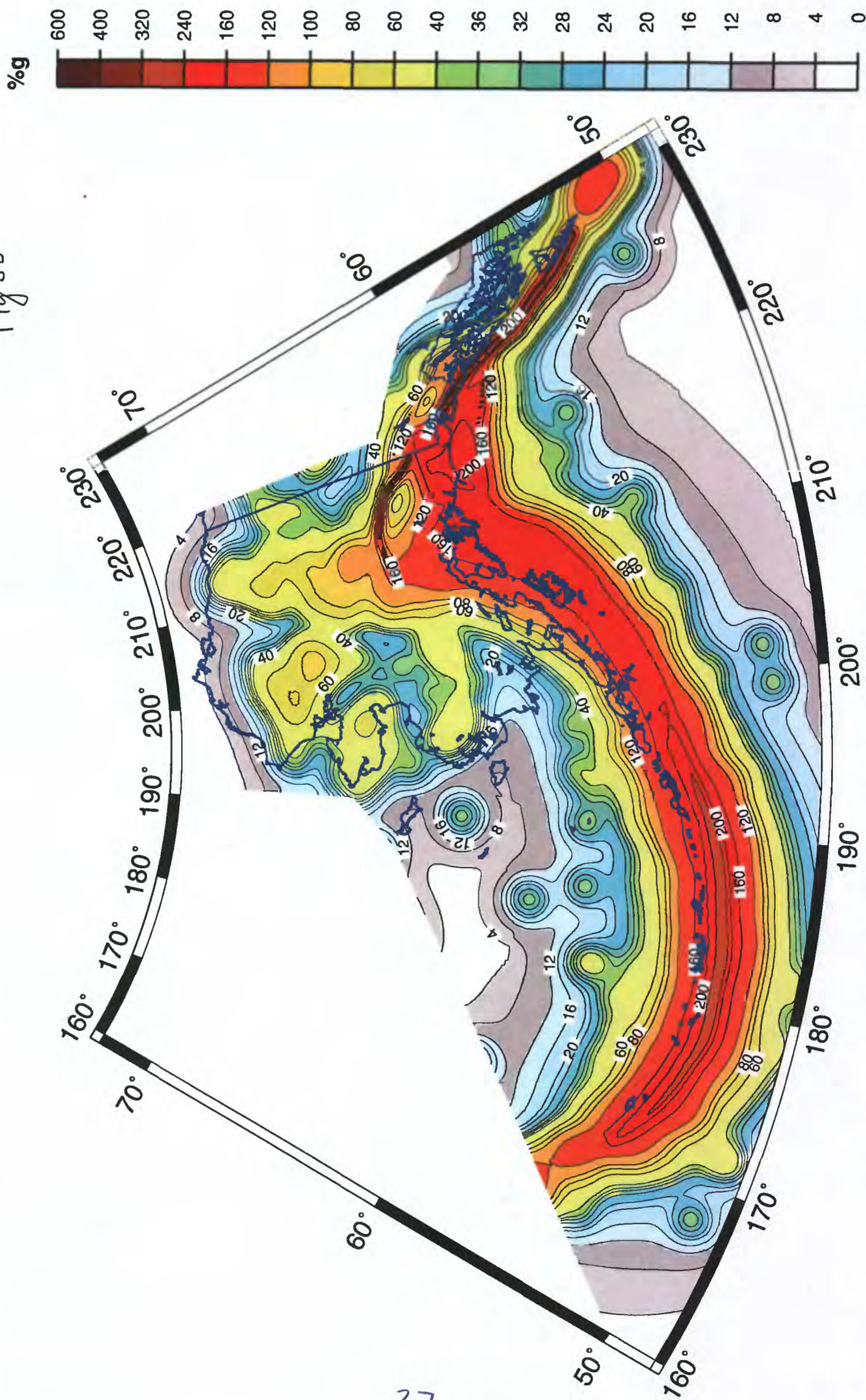
Fig 8a



5 Hz Spectral Acceleration (%g) with 10% Probability of Exceedance in 50 Years

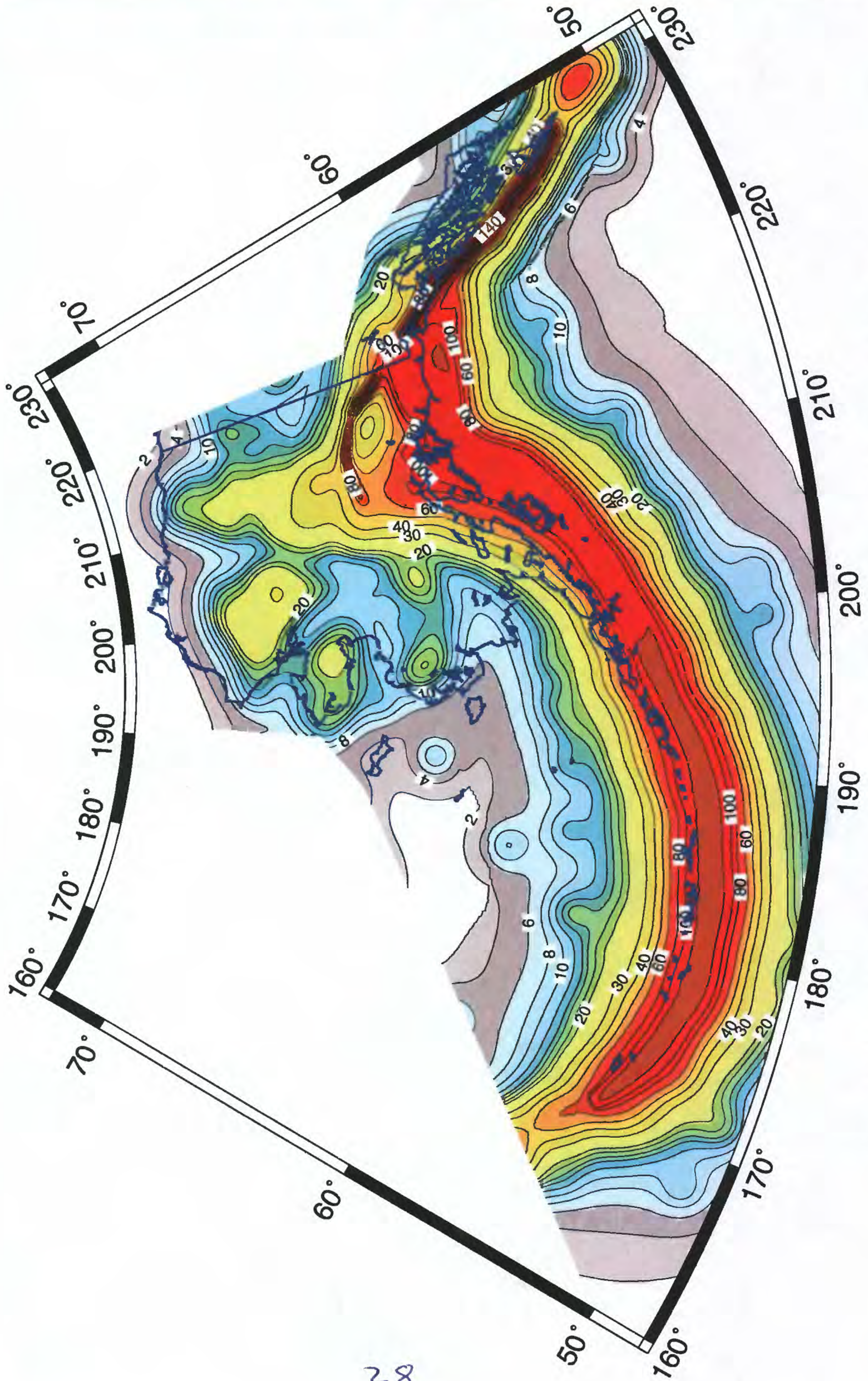
Figure 8a

Fig 8b

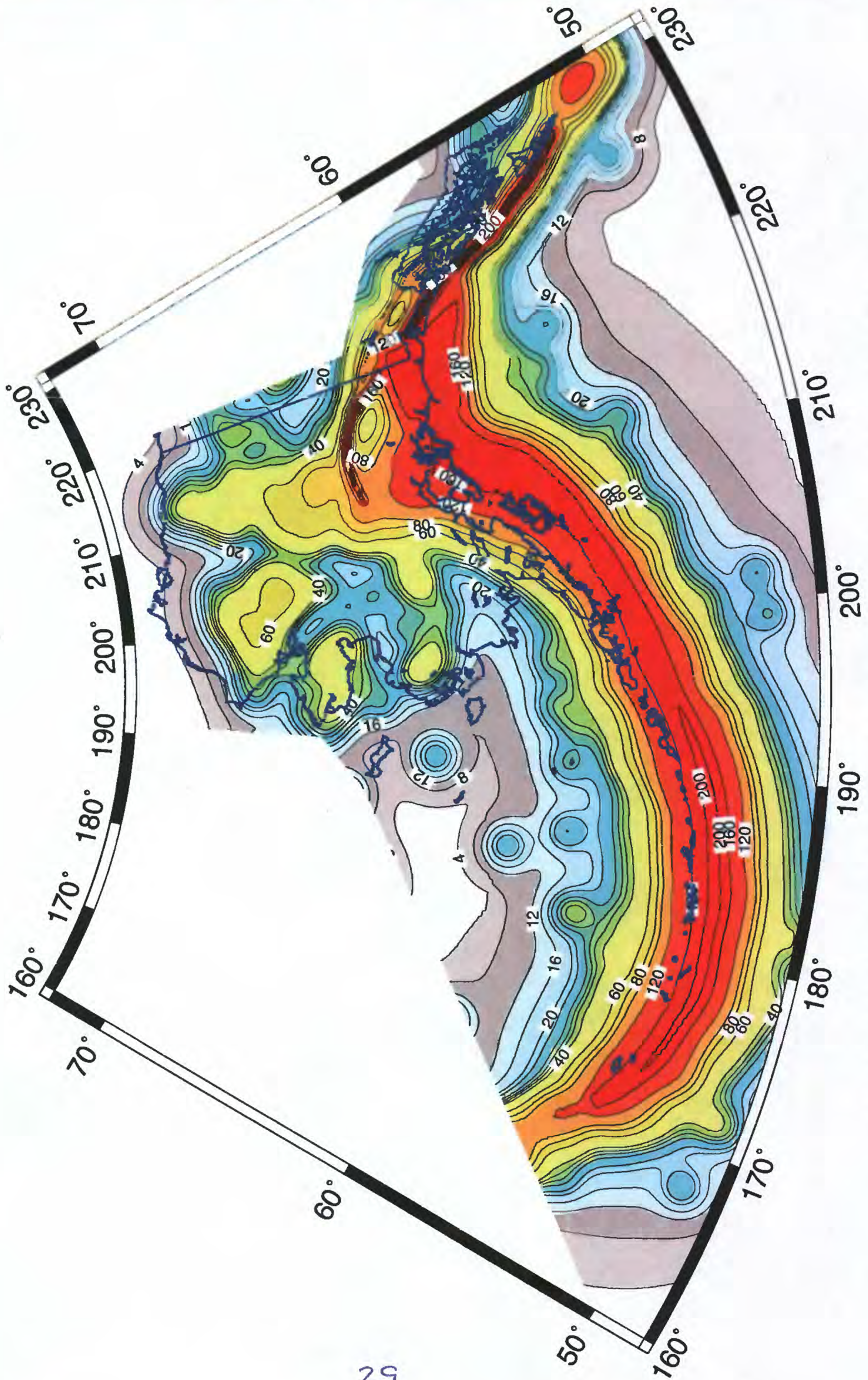


5 Hz Spectral Acceleration (%g) with 2% Probability of Exceedance in 50 Years

Figure 8b

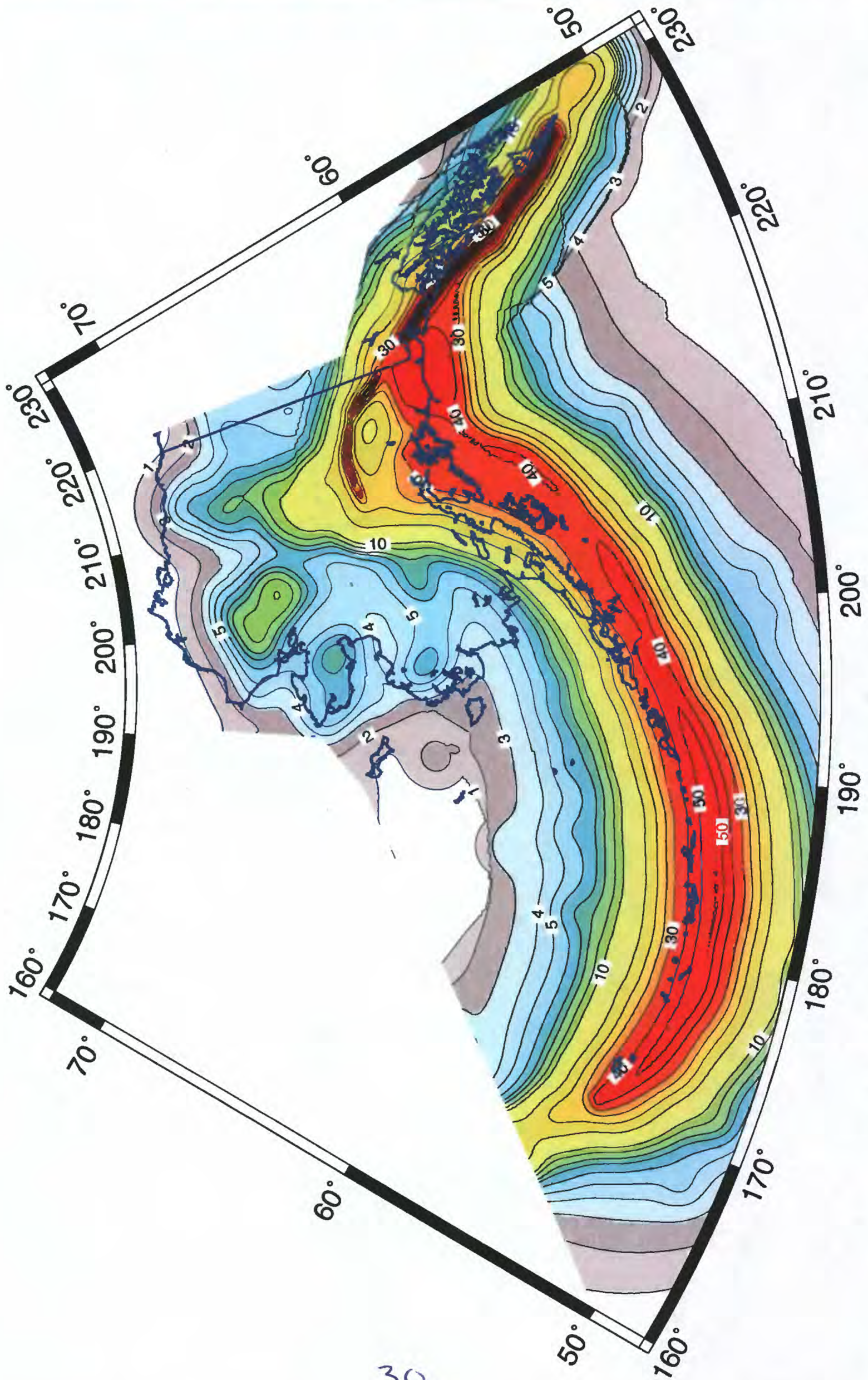
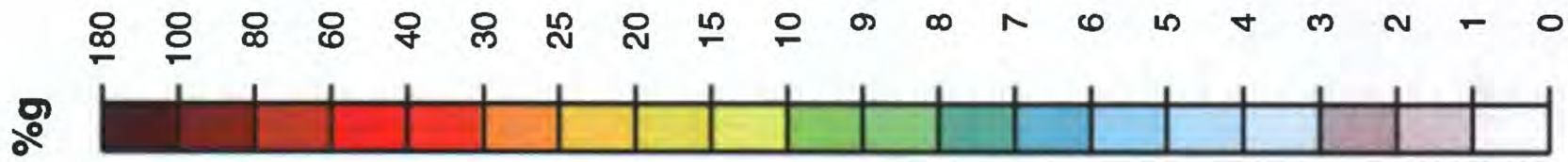


3 Hz Spectral Acceleration (%g) with 10% Probability of Exceedance in 50 Years



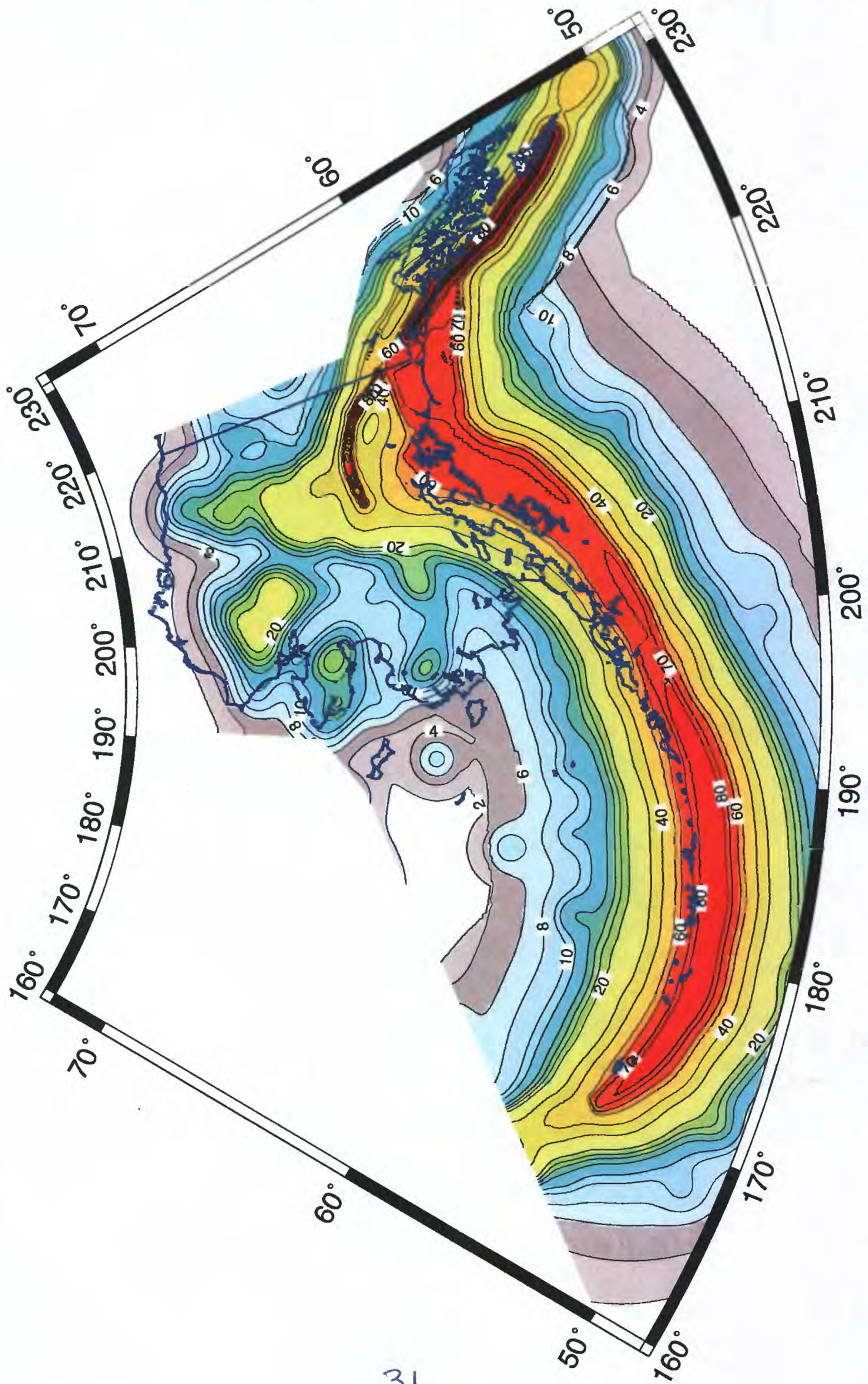
3 Hz Spectral Acceleration (%g) with 2% Probability of Exceedance in 50 Years

Figure 9b



1 Hz Spectral Acceleration (%g) with 10% Probability of Exceedance in 50 Years

Figure 10a



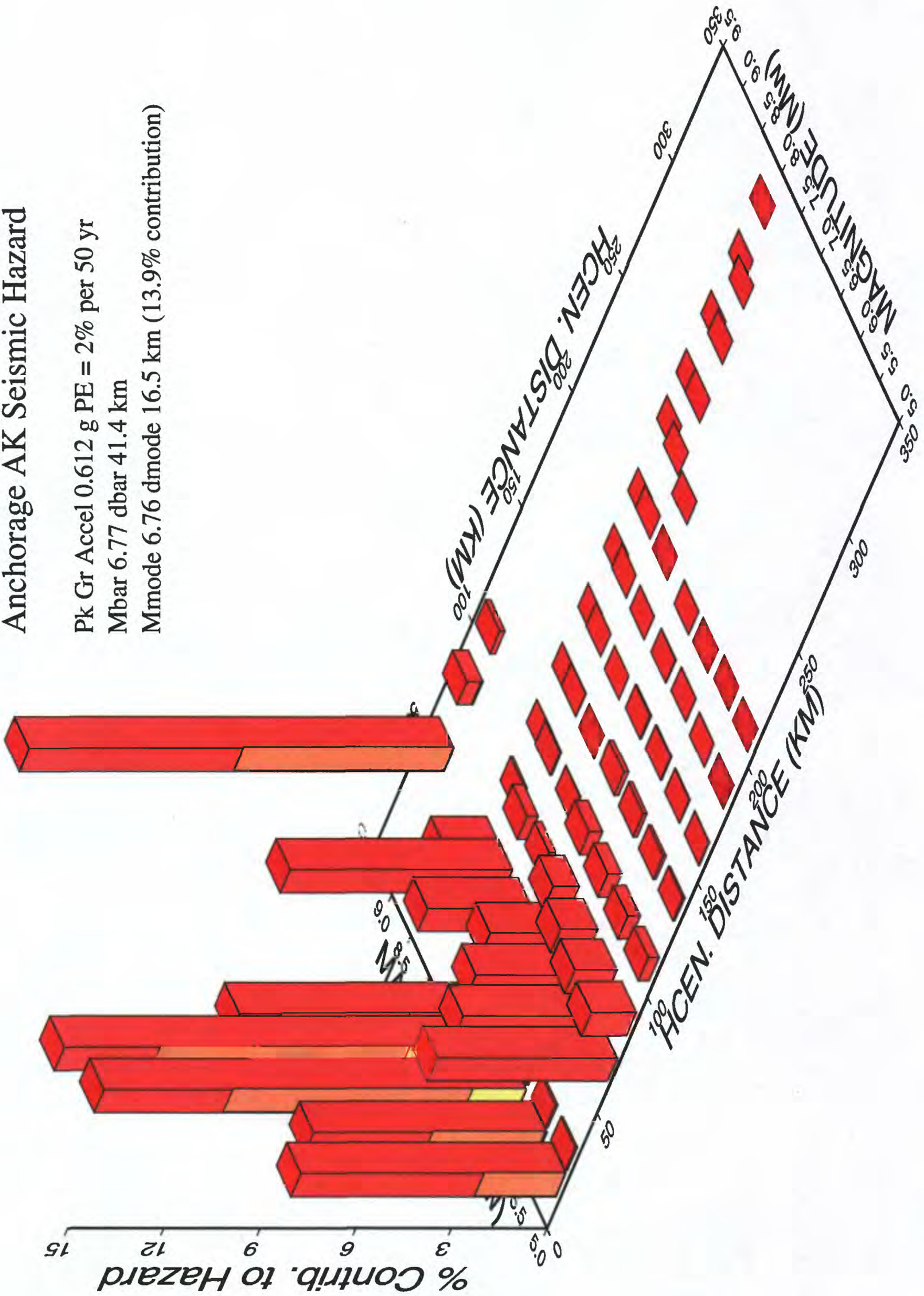
1 Hz Spectral Acceleration (%g) with 2% Probability of Exceedance in 50 Years

# Anchorage AK Seismic Hazard

Pk Gr Accel 0.612 g PE = 2% per 50 yr

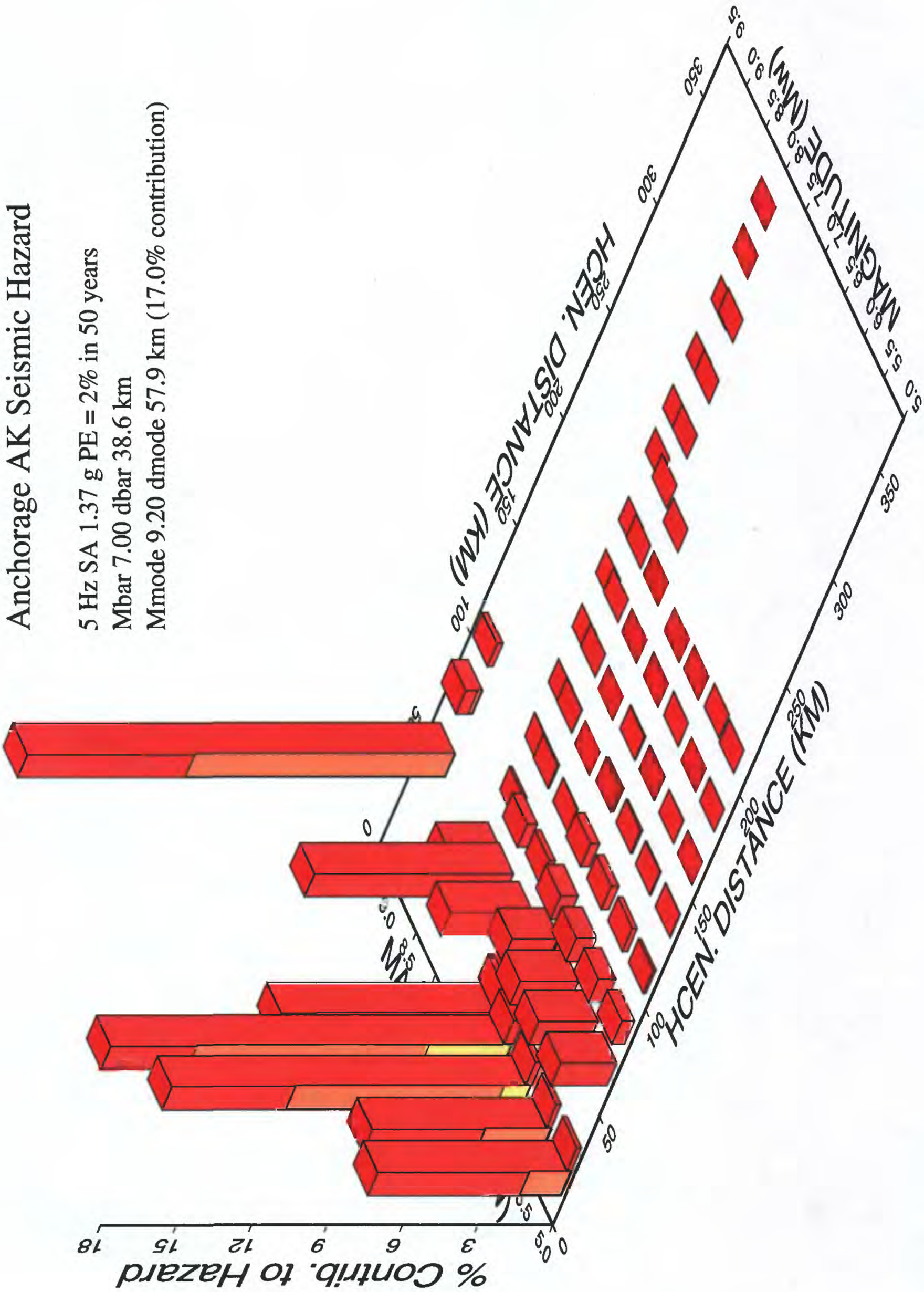
Mbar 6.77 dbar 41.4 km

Mmode 6.76 dmode 16.5 km (13.9% contribution)



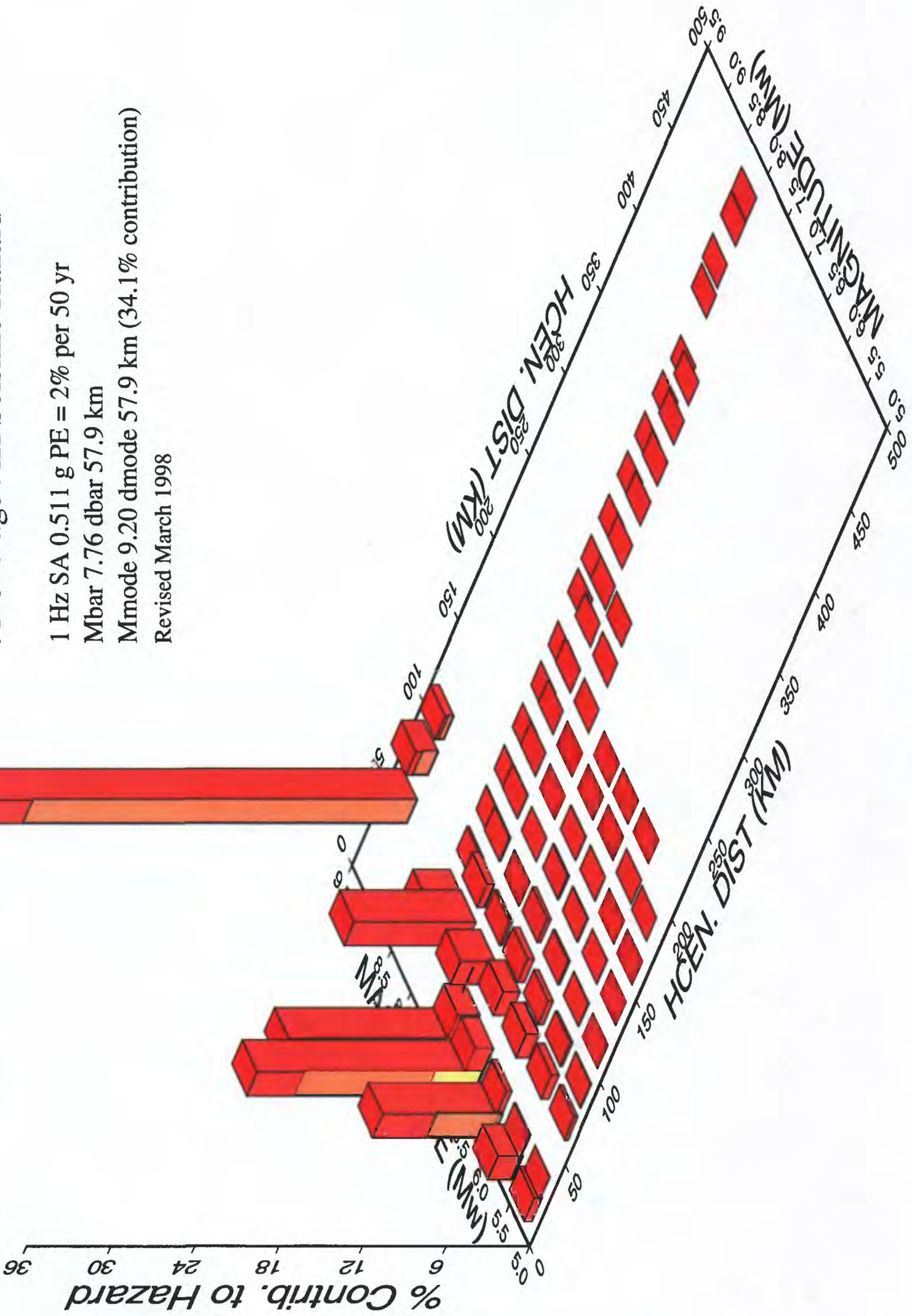
# Anchorage AK Seismic Hazard

5 Hz SA 1.37 g PE = 2% in 50 years  
 Mbar 7.00 dbar 38.6 km  
 Mmode 9.20 dmode 57.9 km (17.0% contribution)



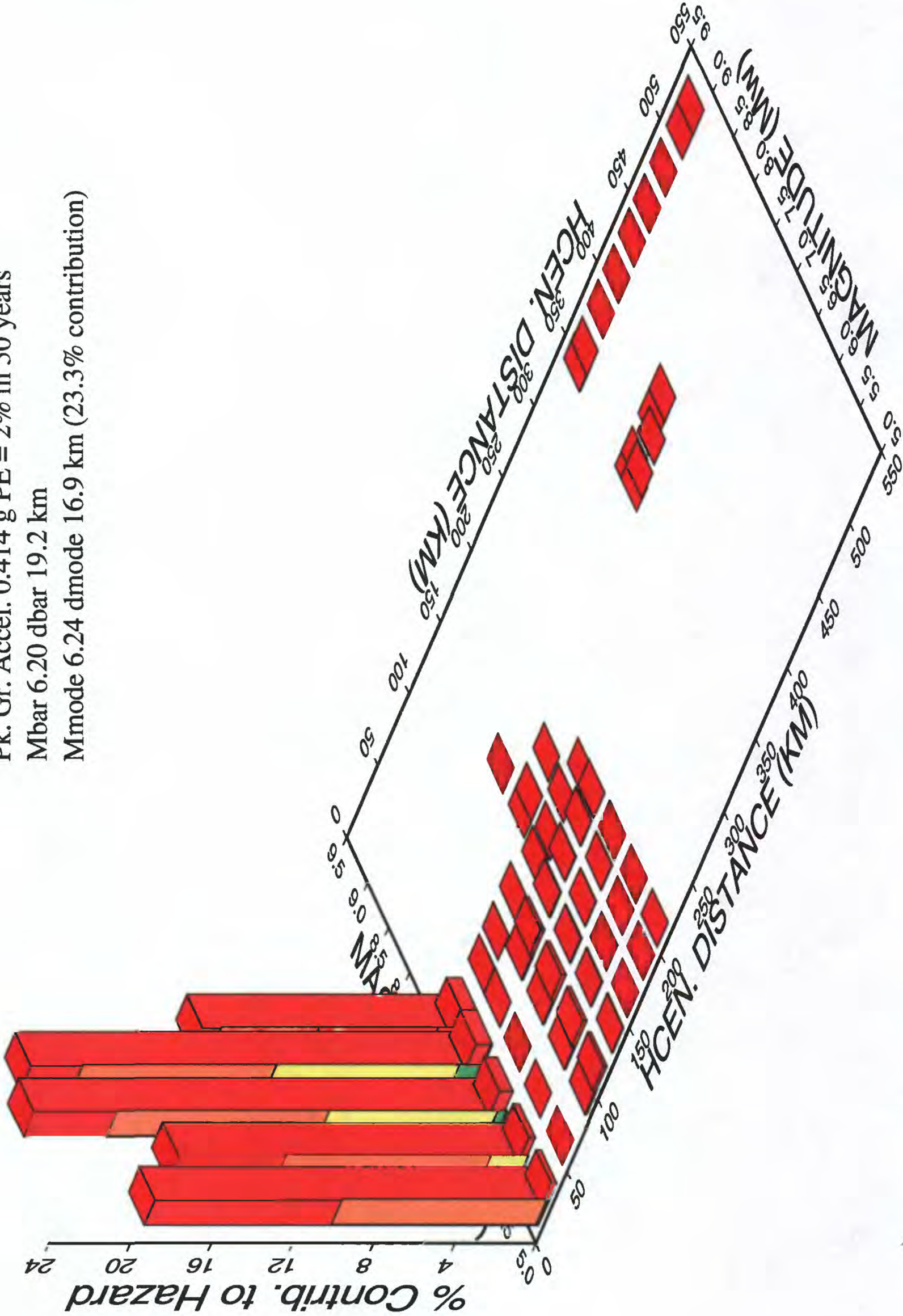
# Anchorage AK Seismic Hazard

1 Hz SA 0.511 g PE = 2% per 50 yr  
 Mbar 7.76 dbar 57.9 km  
 Mmode 9.20 dmode 57.9 km (34.1% contribution)  
 Revised March 1998



# Fairbanks AK Seismic Hazard

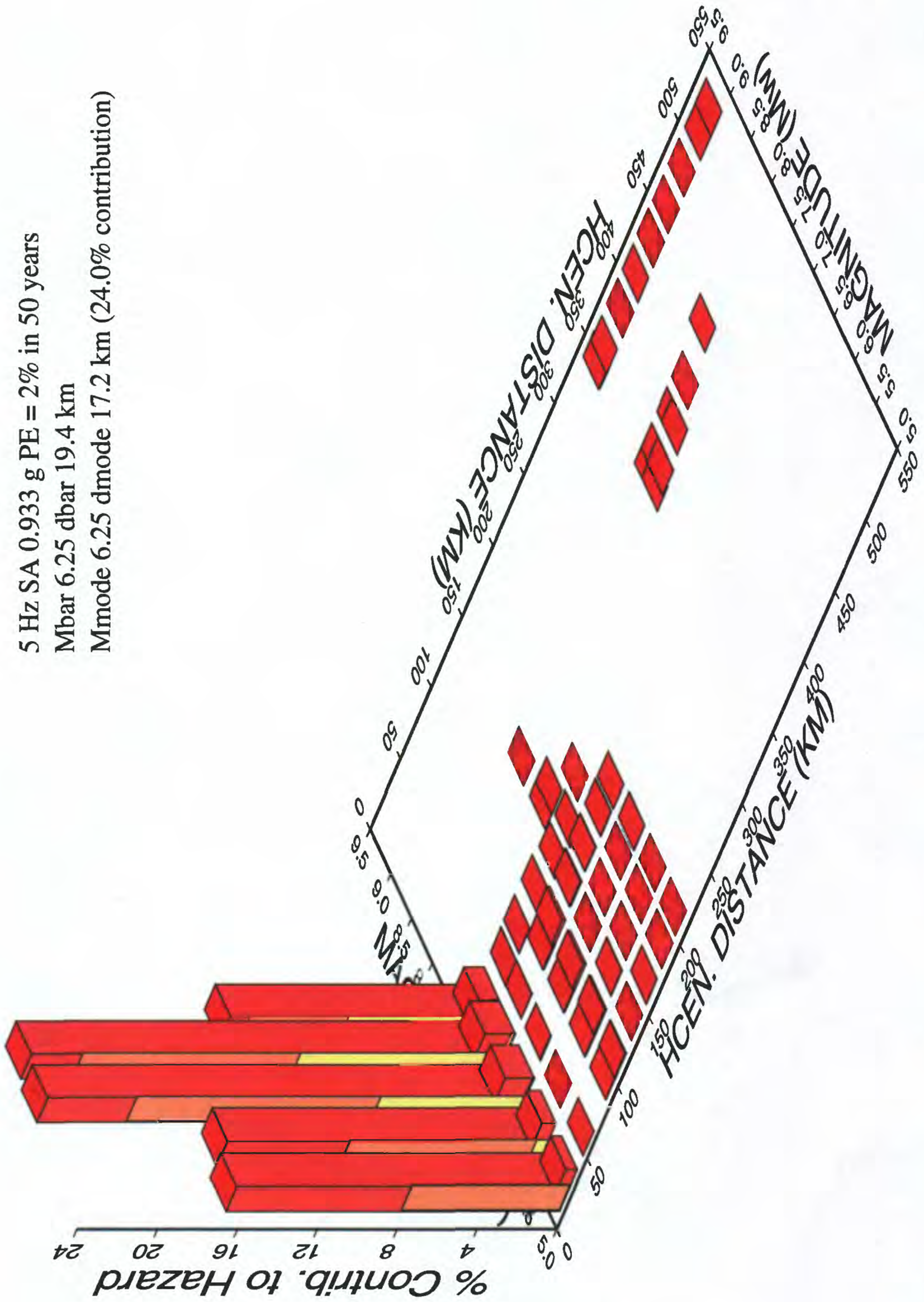
Pk. Gr. Accel. 0.414 g PE = 2% in 50 years  
 Mbar 6.20 dbar 19.2 km  
 Mmode 6.24 dmode 16.9 km (23.3% contribution)



53

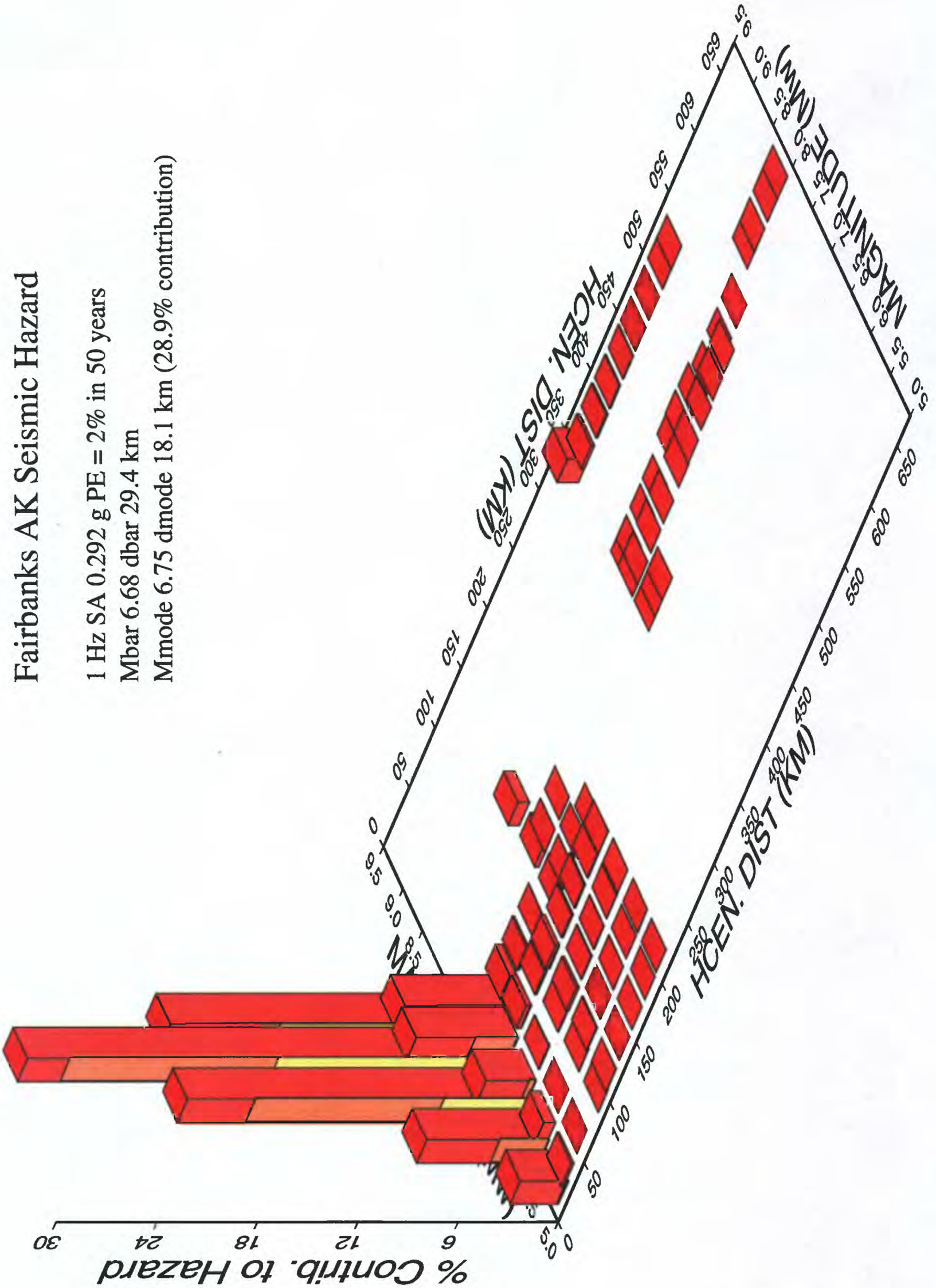
# Fairbanks AK Seismic Hazard

5 Hz SA 0.933 g PE = 2% in 50 years  
 Mbar 6.25 dbar 19.4 km  
 Mmode 6.25 dmode 17.2 km (24.0% contribution)



# Fairbanks AK Seismic Hazard

1 Hz SA 0.292 g PE = 2% in 50 years  
 Mbar 6.68 dbar 29.4 km  
 Mmode 6.75 dmode 18.1 km (28.9% contribution)

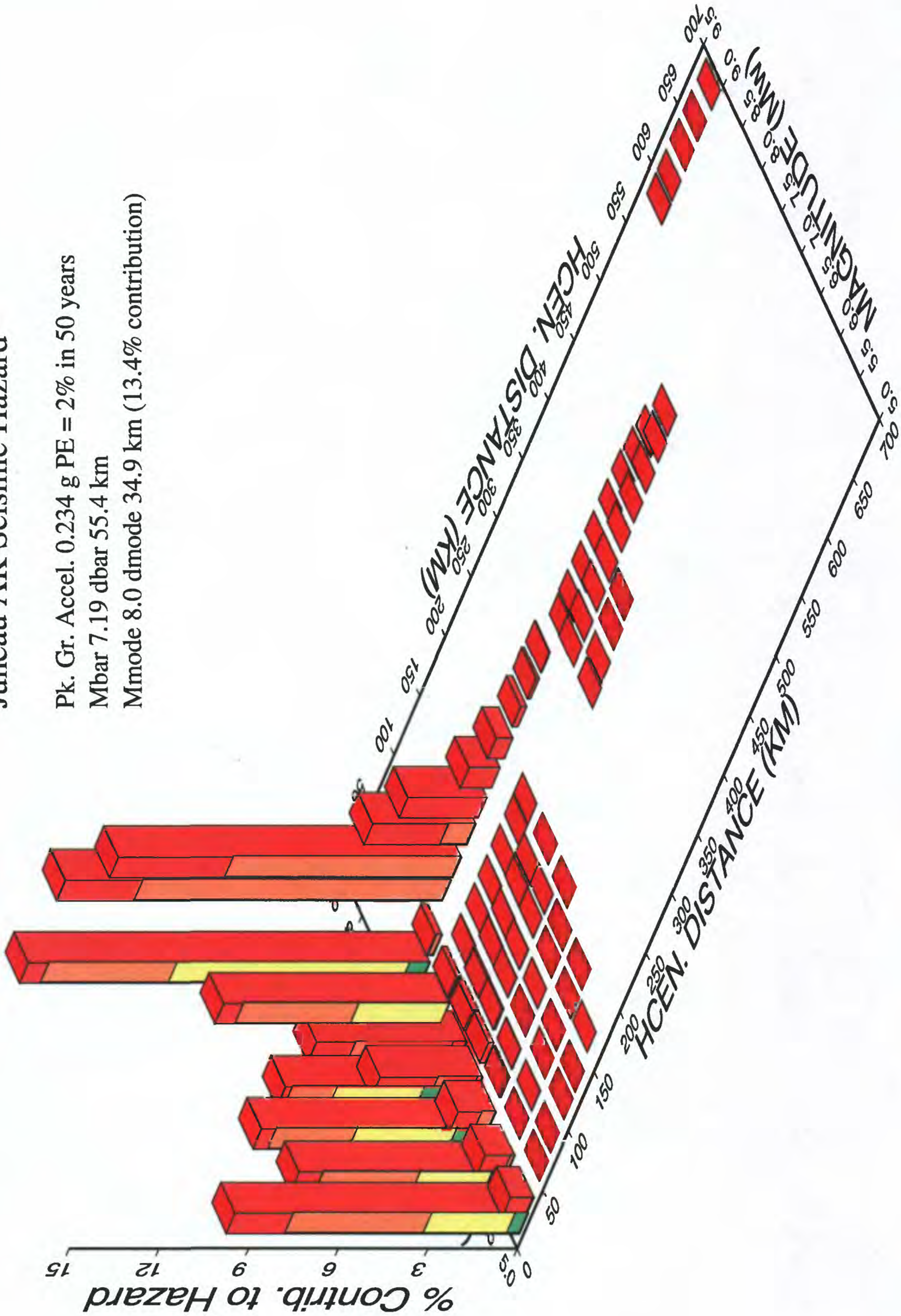


# Juneau AK Seismic Hazard

Pk. Gr. Accel. 0.234 g PE = 2% in 50 years

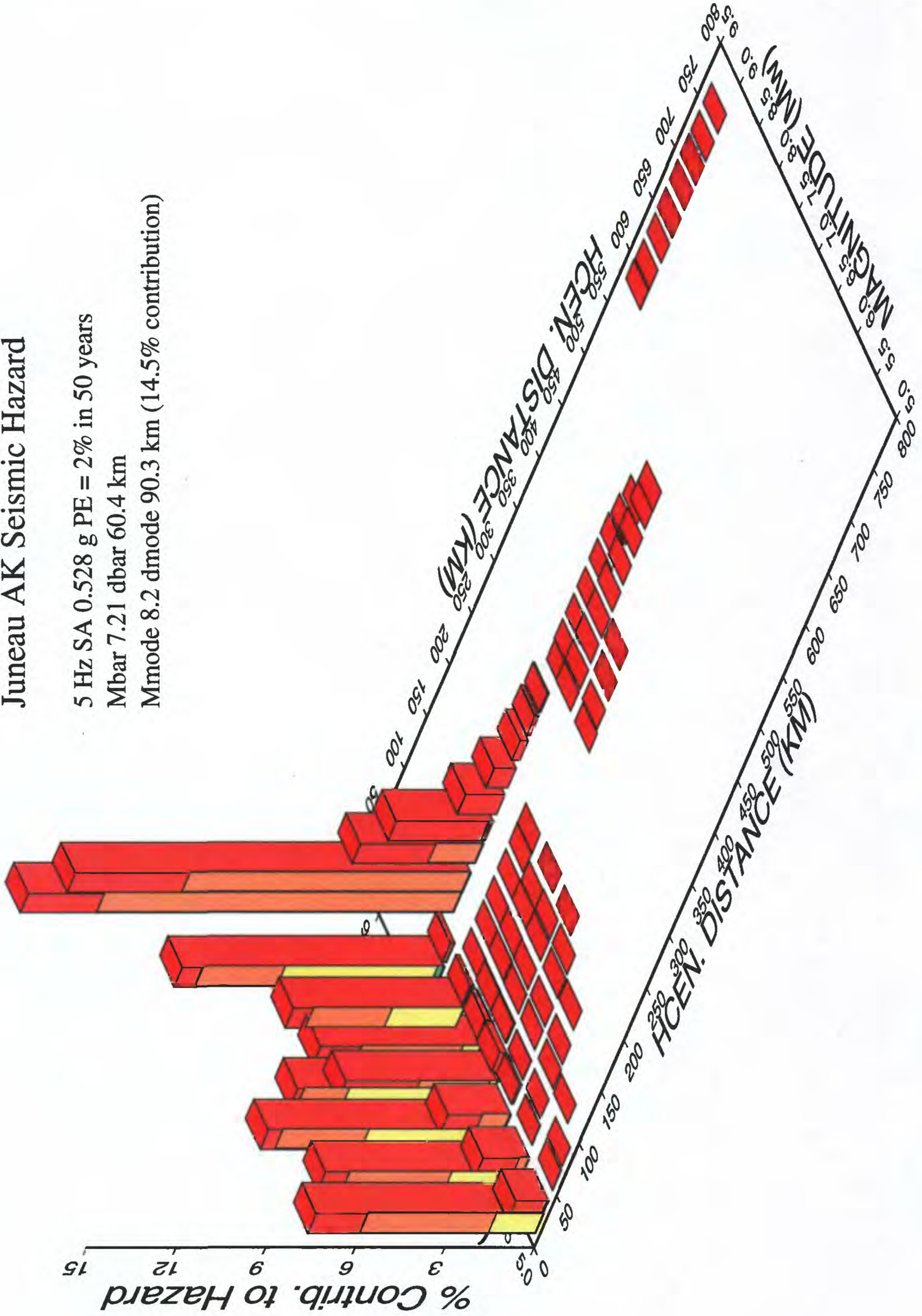
Mbar 7.19 dbar 55.4 km

Mmode 8.0 dmode 34.9 km (13.4% contribution)



# Juneau AK Seismic Hazard

5 Hz SA 0.528 g PE = 2% in 50 years  
 Mbar 7.21 dbar 60.4 km  
 Mmode 8.2 dmode 90.3 km (14.5% contribution)

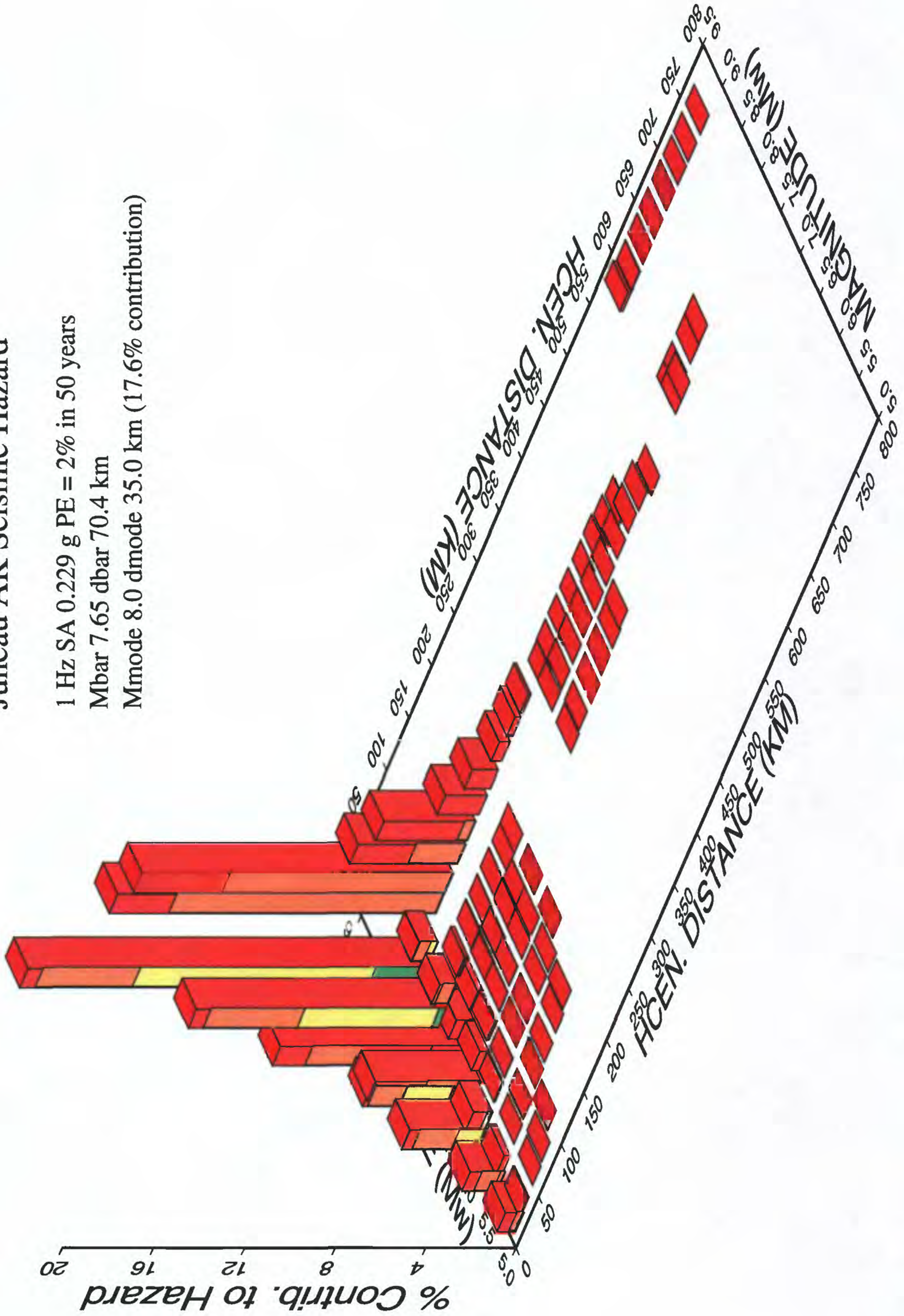


# Juneau AK Seismic Hazard

1 Hz SA 0.229 g PE = 2% in 50 years

Mbar 7.65 dbar 70.4 km

Mmode 8.0 dmode 35.0 km (17.6% contribution)



47

Table 1. Fault Characteristics

| Fault (segment)       | $M_{\text{char}}$ ( $M_{\text{max}}$ ) (from length) | Slip rate (mm/yr) | Recurrence time <sup>1</sup> for characteristic earthquake (years) | Characteristic (A) or Hybrid (B) | References                                       |
|-----------------------|--|-------------------|--|----------------------------------|--|
| Queen Charlotte       | 8.1  | 58                | 130  | A                                | Nishenko and Jacob (1990)                        |
| Fairweather, offshore | 7.9  | 52                | 120  | A                                | Nishenko and Jacob (1990); Plafker et al. (1993) |
| Fairweather, onshore  | 7.8  | 52                | 110  | A                                | Nishenko and Jacob (1990)                        |
| Denali, southeast     | 8.1 <sup>2</sup>                                     | 2                 | 1900   | B                                | Plafker et al. (1993)                            |
| Denali, central       | 8.0  | 10                | 700  | B                                | Plafker et al. (1993)                            |
| Totschunda            | 7.7  | 11.5              | 400  | B                                | Plafker et al. (1993) (See text)                 |
| Castle Mountain       | 7.5 <sup>3</sup>                                     | 0.5               | 5000   | B                                | (See text)                                       |
| Transition            | 8.2  | 10                | 200  | A                                | (See text)                                       |

<sup>1</sup> Recurrence times are estimated from the rate of seismic moment release for earthquakes of the characteristic magnitude required to balance the observed geologic slip rate, and are rounded to two significant figures.

<sup>2</sup> On the basis of length alone the southeast Denali fault would give a magnitude exceeding 8.1. However, there seems to be no historical precedent for a continental, strike-slip fault generating an earthquake with a moment magnitude,  $M_w$ , exceeding 8.1.

<sup>3</sup> On the basis of length alone, the Castle Mountain fault would yield a magnitude of 7.8. In view of the uncertainties of the length, slip rate and other seismic characteristics of the fault, a lower value of 7.5 was adopted. Because this lower estimate leads to more frequent earthquakes, and thus higher estimates of hazard, this is considered an appropriately conservative assumption.

Table 2. Attenuation Relationships

| Source                                | Attenuation Relationship                               | Frequencies        | Weight        |
|---------------------------------------|--|--------------------|---------------|
| Megathrust and Transition Fault       | Youngs et al. (1997) (Interface)                       | pga, 1, 3.33, 5 Hz | 100%          |
| Crustal faults, shallow earthquakes   | Boore et al (1997) NEHRP B/C                           | pga                | 33 1/3 % each |
|                                       | Sadigh et al. (1997) rock                              |                    |               |
|                                       | Campbell and Bozorgnia (1994) soft-rock                |                    |               |
|                                       | Boore et al. (1997)<br>Sadigh et al. (1997)            | 1, 3.33, 5 Hz      | 50 % each     |
| Deep earthquakes (depth= 50-80 km)    | Youngs et al. (1997) (Intraslab; depth fixed at 60 km) | pga, 1, 3.33, 5 Hz | 100%          |
| Deeper earthquakes (depth= 80-120 km) | Youngs et al. (1997) (Intraslab; depth fixed at 90 km) | pga, 1, 3.33, 5 Hz | 100%          |

Table 3. Comparison of Peak Ground Accelerations of  
Current Maps with Thenhaus et al. (1985)  
(%g)

| Location  | Lat.<br>(°N) | Long.<br>(°W) | 10% in 50 years |                     | 2% in 50 years  |                     |
|-----------|--------------|---------------|-----------------|---------------------|-----------------|---------------------|
|           |              |               | Current<br>Map# | Thenhaus<br>et al.* | Current<br>Map# | Thenhaus<br>et al.* |
| Anchorage | 61.2         | 149.9         | 38              | ~45                 | 66              | ~67                 |
| Barrow    | 71.3         | 156.8         | <1              | <4                  | 1               | <4                  |
| Bethel    | 60.8         | 161.8         | 6               | ~6                  | 13              | ~13                 |
| Cold Bay  | 55.2         | 162.7         | 27              | ~15                 | 48              | ~25                 |
| Fairbanks | 64.8         | 147.7         | 21              | ~22                 | 43              | ~37                 |
| Juneau    | 58.3         | 134.4         | 13              | ~10                 | 25              | ~15                 |
| Kodiak    | 57.8         | 152.4         | 46              | ~60                 | 75              | ~65                 |
| Nome      | 64.5         | 165.4         | 9               | ~8                  | 22              | ~15                 |
| Sitka     | 57.1         | 135.3         | 22              | ~40                 | 35              | ~40                 |

# Calculated values

\* Values interpolated visually from published map